NEUTRON SCATTERING STUDIES OF SOLID METHANE

NEUTRON SCATTERING STUDIES OF SOLID METHANE

by

NORMAN THOMAS JOHNSTON

A Thesis

Submitted to the Faculty of Graduate Studies

in Partial Fulfilment of the Requirements

for the Degree

Master of Science

McMaster University

September 1972

MASTER OF SCIENCE (1972) McMASTER UNIVERSITY
(Physics) Hamilton, Ontario

TITLE: Neutron Scattering Studies of Solid Methane

AUTHOR: Norman Thomas Johnston, B.Sc. (University of Manitoba)

SUPERVISOR: Professor M. F. Collins

NUMBER OF PAGES: vii,67

SCOPE AND CONTENTS:

The total scattering cross section of solid methane has been measured for temperatures in the range from 4.2°K to 95°K. An anomalous increase in the total scattering cross section was observed at temperatures below 5°K. The effect is ascribed to conversion between nuclear spin species. Such spin conversion had been indicated by specific heat and NMR measurements; the present results give an independent confirmation of this. Calculations of the equilibrium value of $\langle I(I+1) \rangle$ at 4.2°K give values lower than those obtained in the NMR work. The specimens used in the present work come to spin equilibrium in times much less than 20 minutes. This is less than the value of 90 minutes for pure methane seen by NMR; however, very small amounts of oxygen impurity in the specimen are known greatly to decrease this time.

An abrupt change in the total scattering cross section at the 20°K phase transition is explained by a change in the rotational freedom of the molecules to a more strongly hindered state below the phase transition. In the region

above the transition, the Krieger-Nelkin approximation for the total cross section was fitted to the observed temperature dependence of the cross section, treating the effective mass as a free parameter.

TABLE OF CONTENTS

LIST OF FIGURES

LIST OF TABLES

ACKNOWLEDGEMENTS

I would like to thank my research supervisor, Professor M. F. Collins, for his guidance, encouragement, and kindness throughout the course of this work. His advice and enthusiasm have been greatly appreciated.

I would like to thank Professor J. A. Morrison for his continued interest in this work, and particularly for several enlightening discussions on methane and for the communication of results prior to publication.

I would also like to thank Professor B. N. Brockhouse for allowing me to use the triple-axis spectrometer at the McMaster University reactor to perform these experiments.

To my colleagues in the solid state group at McMaster University; Mr. S. G. Boronkay, Mr. R. R. Dymond, Mr. G. H. Griffin, Mr. W. A. Kamitakahara, Mr. A. Larose, Mr. J. A. Stiles, Dr. H. C. Teh, and Mr. V. K. Tondon go my sincere thanks for their friendship and assistance for the last two years.

I am grateful to McMaster University for financial support in the form of a University teaching assistantship. This work was supported by grants from the National Research Council of Canada.

Finally, I thank Mrs. M. Pope for her expert typing of this thesis.

CHAPTER I

INTRODUCTION

1. Outline of the Thesis

This thesis presents the results of measurements of the total scattering cross section of methane for slow neutrons. The measurements were primarily undertaken to study the conversion between nuclear spin symmetry species thought to occur in methane at low temperatures (Wong et al. 1968; Runolfson et al. 1969; Piott 1971), but during the course of the work it became evident that the temperature dependence of the total scattering cross section could yield information concerning the rotational freedom of the methane molecule in the solid phases.

The first chapter of the thesis provides an introduction to the problems of changes in the relative populations of the three nuclear spin symmetry species in methane and of the degree of molecular rotational freedom in solid methane. A brief account of the experimental evidence concerning these problems is given. The usefulness of neutron total scattering cross section measurements to the study of these problems is indicated.

Chapter two presents the theory of slow neutron scattering. An explicit expression for the dependence of the total scattering cross section of methane on the thermal

average of the nuclear spin quantum number of the molecule is derived. A brief account of the theory of slow neutron scattering from real molecular gases is given.

The third chapter describes the experimental arrangement and the method of making the measurements.

The final chapter presents the results of the experiment. The method of analysis is described, and the results are discussed in terms of spin species conversion and of changes in the rotational freedom of the molecules.

2. Solid Methane

The methane molecule forms a regular tetrahedron with the carbon atom at the centre and the hydrogen atoms at the four apexes (figure I-1). The hydrogen atoms are strongly covalently bonded to the carbon atom by sp^3 hybrid electron orbitals directed along the C-H axes. The structure has high symmetry; the symmetry group of the molecule being T_d. Partly as a result of this, methane molecules interact only through weak Van-der-Waals-type forces.

The methane molecule contains four identical hydrogen nuclei (protons) whose nuclear spins can couple to yield states with total nuclear spin quantum numbers of I = 0, 1 or 2. The Pauli exclusion principle requires that the molecular wavefunction be antisymmetric under the interchange of any two protons. However, because of the T_d symmetry of the methane molecule, the interchange of any two protons is equivalent to the rotation of the molecule about one of the symmetry axes. As a consequence, the nuclear spin states are coupled

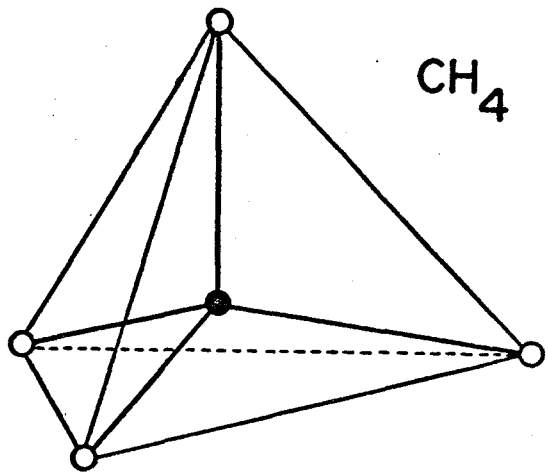

Figure I-1 A molecule of methane. The unfilled circles represent the hydrogen atoms and the filled circle represents the carbon atom. The symmetry group of the molecule is T_d.

to the rotational states in the sense that only certain of the low lying rotational states are available to states of given nuclear spin, the correspondence being: I = 2, J = 0,3,4; I = 1, J = 1,2,3,4; I = 0, J = 2, 4,5 (de Wit and Bloom 1969). The three distinct nuclear spin states of methane are termed meta (I = 2), ortho (I = 1) and para (I = 0) states and are labelled A, T, and E respectively according to the irreducible representations of the group T_d under which they transform. The energy levels of the free methane molecule have both rotational and spin degeneracies.

The moments of inertia about the three principal axes of the methane molecule are equal and methane is therefore termed a spherical top molecule. The moment of inertia is small in value due to the low mass of the proton (see table I-1) and the separation between the J = 0 and J = 1 rotational energy levels is about 14.6°K.

At very low temperatures, a methane molecule will be in the rotational ground state consistent with its nuclear spin state. The crystal field associated with the regular lattice of methane molecules will probably be quite small because of the high symmetry of the molecule. Thus the rotational angular momentum will probably not be quenched and the molecular energy levels will retain their rotational and spin degeneracies. An inhomogeneous magnetic field produced by one hydrogen nucleus at the site of another might mix spin states and produce a slow conversion between nuclear spin species (Bloom 1971). Because of the correspondence between spin and rotational states, such a conversion would change the

TABLE I-1

Selected physical properties of methane

molecular weight (a.m.u.)[a]		16.04
moment of inertia (gm. - $cm.^2$)[b]		5.330×10^{-40}
C-H bond distance (Å)[b]		1.0931
boiling point at one atmosphere pressure (^oK)[c]		111.67
triple point(^oK)[d]		90.675
upper transition temperature (^oK)[d]		20.49
lower transition temperature (^oK)[d,e]		∿8
density at 20.5^oK (gm.-$cm.^3$)[f]		0.522_5
thermal neutron cross sections (barns):[g]		
carbon	σ_{coh}	5.50
	σ_{inc}	∿0.01
	σ_{abs} (1.08Å)	0.003
hydrogen	σ_{coh}	1.79
	σ_{inc}	∿79.7
	σ_{abs} (1.08Å)	0.19
thermal neutron scattering lengths (cm.)[h,i]		
carbon	a	0.610×10^{-12}
hydrogen	$a_{(+)}$	0.538×10^{-12}
	$a_{(-)}$	-2.371×10^{-12}

[a] Handbook of Physics and Chemistry, 49th edition (Chemical Rubber Co., Cleveland, 1968)

[b] Herzberg 1945

Table I-1 (continued)

[c] American Institute of Physics Handbook (McGraw-Hill Co. Ltd., New York, 1957)

[d,e] Colwell, Gill and Morrison 1963, 1962

[f] Tolkachev and Manzhelii (1966)

[g] Hughes and Schwartz 1958

[h] Preston 1962

[i] Bacon 1962

rotational state and result in a reorientation of the molecule with respect to the crystal axes (Bloom and Morrison 1972), as well as changing the energy and degeneracy of the molecular energy level occupied. Such a process would result in rather interesting low temperature properties for solid methane and might conceivably result in the solid being disordered at low temperatures (Alexander and Lerner-Noar 1972).

Methane exists as a gas under normal conditions of temperature and pressure. The boiling point is quite low, being 111.67°K at one atmosphere pressure (see Table I-1). The triple point is 90.675°K (Colwell, Gill and Morrison 1963). Solid methane undergoes a phase transition, characterized by a λ-type anomaly in its heat capacity, at 20.49°K (ibid). Anomalous changes in the thermal expansion coefficient (Manzhelii et al. 1969; Heberlein and Adams 1970), proton spin-lattice relaxation time (de Wit and Bloom 1969), and lattice constant (Greer and Meyer 1969) also occur at the transition. The nature of this transition has not been determined unambiguously in CH_4, although there has been speculation that it may represent an abrupt change in the rotational freedom of the molecules (Pauling 1930) or an order-disorder type reorientation of the methane molecules on the crystal lattice (Katakoa and Yamamoto 1968; Alexander and Lerner-Noar 1972; Press 1972)

X-ray diffraction measurements have shown that the carbon atoms of the methane molecules are arranged on a face-centred cubic lattice throughout the temperature range from 4.2°K to the melting point (Schallamach 1939; Greer and Meyer

1969; Herczeg and Stoner 1971). Thus any structural phase transition can involve only a reorientation of the methane tetrahedra with respect to the crystal axes. Neutron diffraction measurements on solid heavy methane (Press 1972) have shown that its upper phase transition is a transition from a totally orientationally disordered structure to a partially ordered structure, while the lower transition is probably an ordering within the sublattice of disordered molecules of phase II. A similar situation may occur in solid methane with the additional complication that nuclear spin conversion may tend to disorder the molecules (Alexander and Lerner-Noar 1972).

In the temperature region from about $6^{o}K$ to $12^{o}K$ there is a broad excess heat capacity (Colwell, Gill and Morrison 1962, 1963) which has variously been interpreted as a second phase transition (ibid) such as occurs in the deuterated modifications of methane, or as the result of conversion between nuclear spin symmetry species (Hopkins, Donoho, and Pitzer 1967), or as a combination of the two (Piott 1971; Ballik, Gannon and Morrison 1972).

Thus, the three fundamental problems to be investigated in solid methane are:

(1) conversion between nuclear spin species

(2) the degree of rotational freedom of the methane molecules in the various phases

(3) the degree of orientational order in the various phases.

It should be noted that in methane these three problems are very intimately connected.

3. Experimental Studies on Solid Methane

A variety of techniques have been used to study solid methane including heat capacity measurements, proton magnetic resonance, infrared absorption spectroscopy, Raman spectroscopy, X-ray diffraction, neutron inelastic scattering and optical birefringence. The conclusions to be drawn from these studies with respect to the three above problems are not always unambiguous, as similar results have been interpreted rather differently in several instances.

The heat capacity measurements of Colwell, Gill and Morrison (1962, 1963) revealed the existence of a broad anomaly, centred around 8^{o}K which they interpreted as a second phase transition. Their measurements also showed that it was necessary to take account of the existence of nuclear spin species in methane in order to explain the apparent zero-point entropy of solid methane. On the assumption that no conversion occurred between spin species, they found that a trigonal crystalline field produced energy level splittings that would account for their entropy measurements.

The assumption of no conversion between spin symmetry species was criticized by Hopkins, Donoho and Pitzer (1967) who argued that the entire heat capacity anomaly was the consequence of such conversion. In proton magnetic resonance measurements on solid methane at 4.2^{o}K, Wolf and Whitney (1964) had observed a thirty per cent increase in the signal strength with a time constant of the order of 90 minutes; they suggested that this might represent spin species conversion. Hopkins *et al.*

performed similar experiments with methane to which varying concentrations of oxygen impurity had been added and observed time-dependent changes in signal strength. Measurements on pure methane showed no change in signal strength. They argued that the small (<0.005 mole%) amounts of oxygen in the samples studied by Colwell et al. catalyzed the conversion between nuclear spin species and that this had produced the anomaly in the heat capacity.

Frayer and Ewing (1968) observed reversible time-dependent changes in the infrared absorption spectra of methane in argon and krypton matrices. These changes had a time constant of about 90 minutes at $4.2^{\circ}K$ and could be reversed on heating. Furthermore, small amounts of oxygen impurity changed the time constant for the observed peak intensity changes to about three minutes. This strongly suggested that spin conversion occurred in solid methane.

Conclusive evidence for nuclear spin conversion was provided by Wong et al. (1968) who measured the ratio of the proton magnetic resonance signal of methane to that of C^{13} in a methane sample containing a known amount of C^{13}. They found that $\langle I(I+1)\rangle = 3.73 \pm 0.18$ at $4.2^{\circ}K$, rather than the value of 3 that would be obtained in the absence of spin conversion. In other resonance experiments Runolfson et al. (1969) found a value of $\langle I(I+1)\rangle = 5.88 \pm 0.03$ at $1.06^{\circ}K$, showing that the conversion process does not go to completion even at these low temperatures.

During the course of this work, Piott (1971) reported the results of a series of nuclear magnetic susceptibility measurements on solid methane, from which he was able to obtain the equilibrium values of $\langle I(I + 1)\rangle$ as a function of temperature. His data were in good agreement with the above data. Piott proposed an energy level scheme consistent with his data and was able to account for most of the heat capacity anomaly on the basis of spin conversion. However a small residual heat capacity, consistent with a change in orientational order, remained near $8^{\circ}K$. Piott also found that an oxygen impurity of 127 ppm had no effect on the conversion kinetics.

One of the first studies of the rotational freedom of methane molecules in the solid phase was a measurement of the Raman spectra at $78^{\circ}K$ made by Crawford, Welsh and Harrold (1952). The spectrum of the solid at $78^{\circ}K$ was identical to that of the liquid at $112^{\circ}K$. The structure of the spectra of both was consistent with free molecular rotation. Anderson and Savoie (1965) made measurements of the Raman spectra of solid methane at temperatures from $10^{\circ}K$ to $77^{\circ}K$ and concluded that the free molecular rotation in the liquid phase is increasingly hindered in the solid until it becomes librational in character at the upper λ-transition.

Savitsky and Horning (1962) made infrared absorption measurements on thin films of methane above and below the upper λ-transition. They saw no rotational fine structure in the spectra and concluded that there must be a potential barrier of the order of several hundred wavenumbers hindering

the free rotation of the methane molecules at temperatures below 40°K.

Neutron inelastic scattering measurements were made on methane at temperatures of 2.7, 6.5, 18 and 84°K by Stiller and Hautecler (1963a, 1963b) and by Dorner and Stiller (1964, 1965). None of the measurements showed well-defined rotational peaks. The frequency distributions at 2.7, 18 and 84°K were similar in structure, with three peaks occurring at energies less than 13 mev; two of these peaks shifted towards lower energies at low temperatures. Two additional peaks occurred in the 6.5°K frequency distribution. It was not possible to assign the peaks to rotational and lattice vibrational modes. The authors concluded that the free rotation of the molecules was slightly hindered in phase I and somewhat more hindered in phase II. They suggested that methane was still in a transition region at 6.5°K.

A very detailed neutron inelastic scattering study of solid methane was made by Harker and Brugger (1967). They observed little change in the scattering above and below the lower transition temperature, but saw dramatic changes at the upper transition. Below the 20.4°K transition, the elastic scattering peaks were narrow and independent of the momentum transfer Q; above the transition they showed Q-dependent broadening. Also, a peak at an energy transfer at 3 mev which had been present in the 5, 9.1 and 18°K spectra was absent at 22.1°K. Harker and Brugger concluded that the molecules were not freely rotating at 22°K and that the upper λ-transition was not the consequence of the freezing out of free rotational

motion. They claimed that a change from an orientationally disordered phase above 20.4°K to an orientationally ordered phase below was consistent with the narrowing of the elastic peaks. Sköld (1968) explained part of the Q-dependent broadening above 22°K by frequent stepwise reorientations of the molecules.

Kosaly and Solt (1966), Solt (1967), Bajorek et al. (1968) and Janik et al. (1969) made neutron inelastic scattering measurements on methane at 80 and 86°K. Their results showed no discrete rotational peaks. Calculations showed that a free rotational model could not give agreement with their observed differential cross sections. It was necessary to introduce a model with a hindering potential and to include translatory vibrations to fit the data. However, from the similarity of the slopes of total cross section versus wavelength curves measured at 80° and 105°K, Rogalska (1965) concluded that molecular rotations were free at 80°K. The good agreement between the data and a no-phonon, free rotation Krieger-Nelkin (1957) calculation was cited as further evidence of free rotation.

Proton spin-lattice relaxation time measurements by de Wit and Bloom (1969) showed discontinuities at the upper transition, suggesting that orientational ordering was involved in the transition. No discontinuity was observed at the lower transition.

Optical birefringence measurements by Ballik, Gannon and Morrison (1972) indicate that methane becomes weakly

birefringent below 18°K. The birefringence was both temperature and time dependent. The authors note that the effect is consistent with an orientational ordering that can be disordered by spin conversion.

To summarize what has been said, it appears that the existence of spin species conversion in solid methane is reasonably certain, although a confirmation of this by some technique other than proton magnetic resonance is desirable. Molecular rotation may be free or nearly free close to the melting point; the situation is not clear. In the vicinity of the upper phase transition, molecular rotation is strongly hindered. There may be increased hindering below the 20.4°K transition. The upper transition probably involves orientational ordering of the molecules.

For a more detailed discussion of experimental studies of spin conversion and orientational ordering in solid methane, the reader is referred to a review paper by Bloom and Morrison (1972).

4. Neutron Total Cross Section Measurements on Molecular Solids

The measurement of differential scattering cross sections in neutron inelastic scattering studies can yield important information concerning the detailed dynamics of condensed matter, (Brockhouse, Hautecler and Stiller 1964). Measurements of the total neutron cross section gives less detailed information of an integral type over these dynamic properties. Early work in measuring total cross sections concentrated mainly on metallic elements. More recently, the

the technique has been applied to studies of rotational freedom and phase transitions in hydrogenous compounds, particularly the ammonium salts (Rush et al. 1960, 1961, 1962a, 1962b, 1964, 1966; Van Dingenen and Nève de Mevergnies 1964; Janik 1965; Herdade 1968). Rather abrupt changes in the total scattering cross section are seen at phase transitions which involve changes in the rotational freedom of the molecules.

Information on the degree of rotational freedom of molecules in solids can be obtained from the slopes of total cross section versus wavelength and total cross section versus temperature curves, particularly at long wavelengths where the elastic scattering is almost constant and where changes in the total cross section depend primarily on the populations of rotational and vibrational states able to exchange energy with the neutron in energy gain processes.

Because the neutron is a fermion with spin dependent nuclear forces, the total scattering cross section depends upon the average value of the nuclear spin quantum number of the scattering system. Measurements of the total scattering cross section thus permit a direct observation of conversion between nuclear spin symmetry species.

Prior to this work there existed only one report of studies of spin conversion in solids through measurements of neutron total scattering cross sections (Borst et al. 1961). The results, which claimed to show conversion in acetylene and in ice, were in conflict with proton magnetic resonance measurements (Bloom and Jones 1962). A later re-presentation of the

same neutron data for acetylene (Borst 1971) with the addition of error estimates suggests that the conclusions were statistically rather uncertain.

Borst (1971) also claims to have observed spin conversion in solid methane. The data are presented as a graph of cross section versus time at 77°K and upon cooling to 4°K. A decrease in the transmission is cited as evidence of spin conversion. However, for several reasons the conclusion is uncertain:

(1) the transmission of a neutron beam through a methane sample will decrease because of the increase of the sample's density at lower temperatures independently of any change in the cross section.

(2) the transmission data at 77°K show fluctuations which are as large as the fluctuations observed at 4°K that were cited as evidence of a time-dependent cross section.

It is therefore highly questionable as to whether Borst's data show conversion.

Methane seems an ideal system in which to study spin species conversion through neutron total scattering cross section measurements. The incoherent scattering cross section of the hydrogen nuclei is almost two orders of magnitude larger than the coherent cross section of either the carbon or the hydrogen. As we shall show in the next chapter, nuclear spin conversion in methane changes only the incoherent cross section. Thus, the change should be large and easily measurable.

CHAPTER II

THEORY

1. Introduction

Thermal neutrons are uniquely suited as a probe with which to study the static and dynamic properties of condensed matter. Because the de Broglie wavelength of a thermal neutron is comparable with the interatomic spacings in condensed matter, the angular distribution of scattered neutrons yields information concerning the static structure of condensed matter. The energies of thermal neutrons are comparable with those of the elementary excitations which characterize the dynamic behavior of condensed matter, with the result that thermal neutrons undergo energy changes comparable with their initial energies when inelastically scattered. Thus the distribution in energy of inelastically scattered neutrons can yield information on the dynamic behavior of condensed matter. The neutron is a spin one-half particle and consequently scattered neutrons can yield information on the spin state of the scattering system. Furthermore the neutron is a neutral particle and therefore penetrates deeply into a macroscopic sample.

The theory of thermal neutron scattering from molecules has been treated in detail by many authors (Sachs and Teller 1941; Messiah 1951; Zemach and Glauber 1956; Krieger and Nelkin 1957; Griffing 1962; Sinha and Venkataraman 1966; Janik 1968; Parks et al. 1970; Marshall and Lovesy 1971). It should be noted that all the above calculations of the scattering cross section are for molecular gases whereas the experiments described in this thesis were performed on polycrystalline samples of solid methane. The total scattering cross sections calculated for a gas of non-interacting methane molecules are not strictly comparable with the measured total cross sections, which will include phonon scattering and nuclear Bragg scattering from the crystal lattice. However, to first approximation, the scattering of thermal neutrons from polycrystalline methane may be adequately described by the scattering from a gas of methane molecules. The justification of this approximation is twofold:

(1) the neutron scattering from methane is dominated by the incoherent scattering from the hydrogen nuclei, so that the scattering reflects the properties of a single molecule rather than the combined effects of many molecules.

(2) the methane molecules are rather weakly bound in the solid, with the free rotation of the molecules only weakly hindered near the melting point and somewhat more strongly hindered at lower temperatures.

Thus, a non-interacting gas model for solid methane may be reasonable.

For these reasons, and especially because of (1), the crystal structure of solid methane may be neglected to first approximation in calculations of the total cross section. This approximation is necessary since the positions of the hydrogen atoms in various phases of solid methane are not known. Consequently, a first principles calculation of the total cross section for the crystalline solid is impossible. The ultimate justification for the approximation is the reasonable agreement obtained between total cross sections calculated using the gas model and those experimentally measured (Whittemore 1964; Rogalska 1965).

2. The Scattering of Thermal Neutrons from Molecules

The theory presented in this section follows the development of Parks et al. (1970).

We shall consider a molecule composed of N atoms with a Hamiltonian of the form

$$H = -\sum_{j=1}^{N} \frac{\hbar^2}{2M_j} \nabla_j^2 + V(\vec{r}_1, \vec{r}_2, \cdots, \vec{r}_N) \qquad \text{II-1}$$

where M_j is the mass of the j^{th} nucleus and $\vec{r}_j$ is its position vector. The interatomic potential V is assumed to depend only upon the nuclear coordinates. This is the adiabatic approximation which states that the electronic wavefunctions follow changes in the nuclear positions sufficiently rapidly that their motion need not be considered explicitly. The molecular Hamiltonian is assumed to have a complete set of orthonormal eigenstates $U_n(\vec{r}_1, \cdots, \vec{r}_N)$ with associated energies ϵ_n.

The Schrödinger equation for the scattering system consisting of a neutron of momentum $\hbar\vec{k}_o$ and a molecule initially in the state $U_\ell(\vec{r}_1, \cdots, \vec{r}_N)$ is

$$\left[\frac{-\hbar^2}{2m} \nabla_\nu^2 + H + \sum_{j=1}^{N} V_j(|\vec{r}_\nu - \vec{r}_j|) \right]\psi = E\psi \qquad \text{II-2}$$

where m = the mass of the neutron

V_j = the interaction potential between the j^{th} nucleus and the neutron

$\vec{r}_\nu$ = the position vector of the neutron

$\psi = \psi(\vec{r}_\nu, \vec{r}_1, \cdots \vec{r}_N)$ = the wavefunction of the system

and $E = \frac{\hbar^2 k_o^2}{2m} + \varepsilon_\ell$.

Assuming plane wave states for the neutron, the form of the wavefunction at large separations between the neutron and the scatterer is

$$\psi = \exp(i\,\vec{k}_o \cdot \vec{r}_\nu)\, U_\ell(\vec{r}_1, \cdots, \vec{r}_N) + \sum_n f_{\ell n} \exp(i\,\vec{k}\cdot\vec{r}_\nu)\, U_n(\vec{r}_1, \cdots, \vec{r}_N) \qquad \text{II-3}$$

where $f_{\ell n}$ is the scattering amplitude for transitions from the initial molecular state to the final state U_n, and k is defined by

$$\frac{\hbar^2(k_o^2 - k^2)}{2m} = \varepsilon_n - \varepsilon_\ell$$

Expanding the scattered wave in terms of the molecular eigenstates and using the fact that the nuclear potential V_j is very short range, we find

$$f_{\ell n}(\vec{k}_o, \vec{k}) = \frac{m}{2\pi\hbar^2} \int d\vec{r}_\nu \sum_{j=1}^{N} \int d\vec{r}_1 \cdots \int d\vec{r}_N \exp(-i\vec{k}\cdot\vec{r}_\nu)$$

$$U_n^* V_j(|\vec{r}_\nu - \vec{r}_j|)\psi \qquad \text{II-4}$$

The differential cross section of the molecule for transitions to the state $U_n(\vec{r}_1, \cdots, \vec{r}_N)$ is defined as the flux of neutrons with wavevector $\vec{k}$ through the surface element $r^2 d\Omega$ at the position $\vec{r}$ divided by the incident flux and is

$$\frac{d\sigma_{\ell n}}{d\Omega} = \frac{k}{k_o} \left| f_{\ell n}(\vec{k}_o, \vec{k}) \right|^2 \qquad \text{II-5}$$

To evaluate the scattering amplitude $f_{\ell n}$, we approximate the actual short-range nucleus-neutron interaction potential by the Fermi pseudopotential

$$V_j = \frac{2\pi\hbar^2}{m} b_j \delta(\vec{r}_\nu - \vec{r}_j) \qquad \text{II-6}$$

The parameter b_j is the bound scattering length of the j^{th} nucleus. In the first Born approximation, the Fermi pseudopotential correctly gives the observed s-wave scattering of low energy neutrons from a single bound nucleus.

Replacing the wavefunction ψ in equation II-3 by the first Born approximation value of

$$\psi(\vec{r}_\nu, \vec{r}_1, \cdots, \vec{r}_N) = \exp(i\vec{k}_o \cdot \vec{r}_\nu)\, U_\ell(\vec{r}_1, \cdots, \vec{r}_N) \qquad \text{II-7}$$

the scattering amplitude becomes

$$f_{\ell n}(\vec{k}_o, \vec{k}) = \sum_{j=1}^{N} b_j \int d\vec{r}_1 \cdots \int d\vec{r}_N\, U_n^*(\vec{r}_1, \cdots, \vec{r}_N) \exp(i\vec{Q}\cdot\vec{r}_j)$$

$$U_\ell(\vec{r}_1, \cdots, \vec{r}_N)$$

$$= \langle n | \sum_{j=1}^{N} b_j \exp(i\vec{Q}\cdot\vec{r}_j) | \ell \rangle \qquad \text{II-8}$$

where $\hbar\vec{Q} = \hbar\vec{k}_o - \hbar\vec{k}$

The experimentally observed cross section is an average over the thermal equilibrium distribution of states, so that

$$\frac{d\sigma}{d\Omega} = \frac{k}{k_o} \sum_{\ell} g_{\ell} \left| \langle n | \sum_{j=1}^{N} b_j \exp(i \vec{Q}\cdot\vec{r}_j) | \ell \rangle \right|^2 \qquad \text{II-9}$$

where

$$g_{\ell} = \frac{\exp(-\varepsilon_{\ell} / k_B T)}{\sum_{\ell} \exp(-\varepsilon_{\ell}/k_B T)} \qquad \text{II-10}$$

is the statistical weight of the initial state $|\ell\rangle$.

The double differential cross section, defined as the flux of neutrons in the energy range dE at a final neutron energy E scattered through the surface area $r^2 d\Omega$ located at the position $\vec{r}$ divided by the incident flux, is

$$\frac{d^2\sigma}{d\Omega dE} = \frac{k}{k_o} \sum_{\ell,n} g_{\ell} \left| \langle n | \sum_{j=1}^{N} b_j \exp(i \vec{Q}\cdot\vec{r}_j) | \ell \rangle \right|^2 \delta(E_o + \varepsilon_{\ell} - E - \varepsilon_n) \qquad \text{II-11}$$

The basic problem in all cross section calculations is the evaluation of the matrix elements in equations II-9 and II-11.

For a rigid array of N nuclei at positions $\vec{r}_j$, the differential cross section separates (Marshall and Lovesey 1971)

$$\frac{d\sigma}{d\Omega} = \frac{d\sigma}{d\Omega}_{coh} + \frac{d\sigma}{d\Omega}_{inc} \qquad \text{II-12}$$

where the coherent cross section is

$$\left(\frac{d\sigma}{d\Omega}\right)_{coh} = |\bar{b}|^2 \left| \sum_{j=1}^{N} \exp(i \vec{Q}\cdot\vec{r}_j) \right|^2 \qquad \text{II-13}$$

and the incoherent cross section is

$$\left(\frac{d\sigma}{d\Omega}\right)_{inc} = N(\overline{|b|^2} - |\bar{b}|^2) \qquad \text{II-14}$$

From equations II-13 and II-14 we see that in coherent scattering there is strong interference between waves scattered from different nuclei with the result that coherent scattering in a solid occurs strongly only when certain geometric constraints are satisfied (Bragg's law) whereas in incoherent scattering there is no interference and the scattering is more isotropic.

Incoherent scattering has its origin in the random variations of the scattering potential throughout the scattering system. These variations from the mean scattering potential have two sources:

(1) the existence of isotopes of the same element with different scattering lengths

(2) the spin dependence of the neutron-nucleus interaction.

It is the latter with which we are interested.

The scattering system consisting of a thermal neutron interacting with a nucleus of spin I can form two possible states with total spin quantum numbers of $I + \frac{1}{2}$ or $I - \frac{1}{2}$. The neutron-nucleus interactions, and thus the scattering lengths, are different for each of these states.

We denote the bound scattering lengths corresponding to angular momentum states with quantum numbers of $I \pm \frac{1}{2}$ by $b_{(+)}$ and $b_{(-)}$ respectively. The spin dependence of the neutron-nucleus interaction can then be included in our formalism by introducing an effective scattering length (Gurevich and Tarasov 1968).

$$\beta_j = \frac{I_j + 1 + 2(\vec{I}_j \cdot \vec{s}) b_{j(+)}}{2I_j + 1} + \frac{I_j - 2(\vec{I}_j \cdot \vec{s}) b_{j(-)}}{2I_j + 1} \qquad \text{II-15}$$

where $\vec{I}_j$ is the spin operator of the j^{th} nucleus and $\vec{s}$ is the spin operator of the neutron ($|\vec{s}| = \frac{1}{2}$)

Using the effective scattering length II-15 in equation II-9 for the case where both the incident neutron beam and the target nuclei are unpolarized, we find

$$\frac{d\sigma}{d\Omega} = b_{coh}^2 + b_{inc}^2 \qquad \text{II-16}$$

where

$$b_{coh} = \frac{I + 1}{2I + 1} b_{(+)} + \frac{I}{2I + 1} b_{(-)} \qquad \text{II-17}$$

and

$$b_{inc} = \frac{[I(I + 1)]^{\frac{1}{2}}}{2I + 1} (b_{(+)} - b_{(-)}) \qquad \text{II-18}$$

We see from II-17 and II-18 that should $b_{(+)}$ and $b_{(-)}$ be of comparable magnitude but opposite sign, then the scattering cross section would be dominated by the incoherent term and would reflect the value of the nuclear spin.

3. The Elastic Scattering of Thermal Neutrons from Methane

We shall now apply the formalism of the preceding section to a calculation of the elastic scattering cross section of methane. Equation II-9, modified to take account of nuclear spin, forms the starting point

$$\frac{d\sigma}{d\Omega} = \frac{k}{k_o} \sum_{\ell} g_{\ell} \left| \langle n | \sum_{j=1}^{N} \beta_j \exp(i \vec{Q}\cdot\vec{r}_j) | \ell \rangle \right|^2$$

If $|\vec{Q}\cdot\vec{r}_j| \ll 1$, we can expand the exponential in a power series and retain only the first term, whence

$$\frac{d\sigma}{d\Omega} = \frac{k}{k_o} \sum_{\ell} g_{\ell} \left| \langle n | \sum_{j=1}^{N} \beta_j | \ell \rangle \right|^2 \qquad \text{II-19}$$

Because the carbon atom position coincides with the molecular centre of mass $|\vec{r}_j|$ is the carbon-hydrogen separation, 1.0931Å. We therefore require that $Q \ll 0.913 \text{Å}^{-1}$ for the above approximation to be valid. For elastic scattering, this corresponds to requiring that the incident wavelength $\lambda_o \gg 7$Å.

The hydrogen nuclei in methane each have a spin quantum number of one-half and can couple to form a total spin state with spin quantum numbers of I = 0,1 or 2. The population factor g_{ℓ} in equation II-19 then refers to the equilibrium distribution of spin species at the temperature of interest, and will be designated g_I. The carbon atom has no nuclear spin.

Substituting for the effective scattering lengths in II-19, we obtain for a molecule of total spin quantum number I,

$$\frac{d\sigma}{d\Omega}_I = \sum_{i,j=1}^{4} \left[b_{coh}^2 + \frac{4b_{coh}(b_{(+)} - b_{(-)})}{2I_i + 1} \langle \vec{s}\cdot(\vec{I}_i + \vec{I}_j) \rangle \right.$$

$$\left. + \frac{4(b_{(+)} - b_{(-)})^2}{(2I_i + 1)^2} \langle (\vec{s}\cdot\vec{I}_i)(\vec{s}\cdot\vec{I}_j) \rangle \right]$$

$$+ 2 \sum_{i=1}^{4} b_c \left(b_{coh} + 2\frac{(b_{(+)} - b_{(-)})}{2I_i + 1} \langle \vec{s}\cdot\vec{I}_i \rangle \right)$$

$$+ b_c^2 \qquad \text{II-20}$$

where b_{coh} is as defined in equation II-17 and b_c is the scattering length for the carbon nucleus.

For unpolarized incident neutrons, the first and last expectation values are zero. Since the spins at the various hydrogen nuclei are correlated, the second term may be rewritten as

$$\sum_{i,j=1}^{4} \langle (\vec{s}\cdot\vec{I}_i)(\vec{s}\cdot\vec{I}_j) \rangle = \langle \left(\sum_{i=1}^{4} \vec{s}\cdot\vec{I}_i \right) \left(\sum_{j=1}^{4} \vec{s}\cdot\vec{I}_j \right) \rangle$$

$$= \langle (\vec{s}\cdot\vec{I})^2 \rangle$$

$$= \tfrac{1}{4} I(I + 1) \qquad \text{II-21}$$

where we have used the commutation properties of the $\vec{s}$ operator (Messiah 1966). Using the fact that $I_i = \frac{1}{2}$, equation II-20 becomes

$$\frac{d\sigma}{d\Omega}_I = 16 b_{coh}^2 + \tfrac{1}{4}(b_{(+)} - b_{(-)})^2 I(I + 1) + 8 b_{coh} b_c + b_c^2 \qquad \text{II-22}$$

and the total elastic scattering cross section is

$$\sigma = 4\pi \sum_{I=0}^{2} g_I \left(\frac{d\sigma}{d\Omega}\right)_I \qquad \text{II-23}$$

Using the known values of the free hydrogen scattering lengths $a_{(+)}$ and $a_{(-)}$ (table I-1), and noting that the bound atom scattering lengths are related to the free atom scattering length by (Gurevich and Tarasov 1968)

$$b_{(\pm)} = \frac{1 + 1/M}{1 + 1/M_{tot}} a_{(\pm)} \qquad \text{II-24}$$

where M is the mass of the nucleus and M_{tot} is the total mass of the scattering complex, we may calculate the total elastic cross section at any temperature T provided we know the equilibrium distribution of spin states.

Now at any temperature, we have

$$\langle I(I + 1)\rangle = 6g_A(T) + 2g_T(T) \qquad \text{II-25}$$

where we have designated the I = 2,1 and 0 states by their symmetry labels A, T and E. At very high temperatures the ratio of A:T:E species is 5:9:2 so that $\langle I(I + 1)\rangle = 3$, while at absolute zero all the molecules belong to the A species and $\langle I(I + 1)\rangle = 6$. At very low temperatures we have approximately

$$g_A + g_T = 1$$

so that population factors as well as $\langle I(I + 1)\rangle$ can be deduced from cross section measurements.

Slightly different numerical results for the total elastic cross section are obtained depending on whether one considers the scattering complex to which the nuclei are bound

to be the whole crystal or a single methane molecule. The results for both cases are presented in table II-1. In both cases the calculated cross sections are slightly lower than those measured at long wavelengths (Rogalska 1965).

Table II-1

Calculated values of the total elastic scattering cross-section of methane in the long wavelength limit. The subscript "molecule" refers to the case in which the nuclei were considered to be bound in a single molecule, while the subscript "crystal" refers to the case in which the nuclei were considered to be bound in a macroscopic crystal.

$\langle I(I+1) \rangle$	$\sigma_{molecule}$ (barns)	$\sigma_{crystal}$ (barns)
3.0	289.7	327.0
3.1	299.0	337.6
3.2	308.5	348.2
3.3	317.9	358.9
3.4	327.3	369.5
3.5	336.7	380.1
3.6	346.1	390.8
3.7	355.6	401.4
3.8	365.0	412.0
3.9	374.4	422.7
4.0	383.8	433.3
4.1	393.2	443.9
4.2	402.7	454.6
4.3	412.1	465.2
4.4	421.5	475.8
4.5	430.9	486.5
4.6	440.3	497.1
4.7	449.8	507.7
4.8	459.2	518.4
4.9	468.6	529.0
5.0	478.0	539.7
5.1	487.4	550.3
5.2	496.9	560.9
5.3	506.3	571.6
5.4	515.7	582.2
5.5	525.1	592.8
5.6	534.5	603.5
5.7	544.0	614.1
5.8	553.4	624.7
5.9	562.8	635.4
6.0	527.3	646.0

From the results given in table II-1 we see that conversion between different nuclear spin species produces a large change in the cross section, the cross section doubling if complete conversion to the A symmetry species occurs. Using the value of $\langle I(I+1)\rangle$ of 3.73 at 4.2°K (Wong et al. 1968) we expect to see a 15-20% increase in the slow neutron total elastic scattering cross section upon rapid cooling to 4.2°K.

4. Thermal Neutron Scattering from Real Molecular Gases

The calculation of the preceding section gave values for the total cross section which were somewhat smaller than the experimentally measured values because it neglected inelastic scattering from the rotational and vibrational excitations in the solid. A calculation of the total scattering cross section of a molecular gas which includes both elastic and inelastic contributions requires the evaluation of the matrix elements of equation II-11, where the initial and final state wavefunctions depend upon the vibrational, rotational, translational, spin and electronic states of the molecule. Zemach and Glauber (1956) were able to simplify the evaluation of the matrix elements by recasting the problem in an operator formalism which avoided "all explicit use of molecular wavefunctions".

The introduction of the Fourier integral representation of the energy-conserving δ-function

$$\delta(E_o - E - \hbar\omega) = \frac{1}{2\pi\hbar}\int_{-\infty}^{\infty} \exp(i\omega t)\exp[i(E_o - E)t]\,dt \qquad \text{II-26}$$

permitted a summation over final states. With the use of Heisenberg time-dependent operators

$$\vec{r}_j(t) = \exp(i\,Ht)\ \vec{r}_j\ \exp(-iHt) \qquad \text{II-27}$$

where H is the molecular Hamiltonian, the double differential cross section became

$$\frac{d^2\sigma}{d\Omega dE} = \frac{1}{2\pi\hbar}\ \frac{k}{k_o}\int \exp(-i\omega t)\, I(\vec{Q},t)\, dt \qquad \text{II-28}$$

where $I(\vec{Q},t)$ is the intermediate scattering function

$$I(\vec{Q},t) = \sum_{i,j} \langle \ell | b_i\ b_j\ \exp\left[i\vec{Q}\cdot\vec{r}_i(t)\right]\ \exp\left[-i\vec{Q}\cdot\vec{r}_j(0)\right] | \ell \rangle_T \qquad \text{II-29}$$

where the subscript T indicates a thermal average. For certain simple systems, such as vibrating nuclei, the intermediate scattering function is easily evaluated by operator techniques.

The matrix elements in II-29 separate naturally into direct (i = j) and interference (i ≠ j) terms. The evaluation of the direct terms is considerably simplified by defining an effective Hamiltonian

$$H = \exp(i\vec{Q}\cdot\vec{r}_i)\ H(\vec{p}_i,\ \vec{r}_i)\ \exp(-i\vec{Q}\cdot\vec{r}_i)$$

$$= H(\vec{p}_i - \vec{Q}, \vec{r}_i) \qquad \text{II-30}$$

where $\vec{p}_i$ is the momentum canonically conjugate to $\vec{r}_i$. Using such a Hamiltonian, Zemach and Glauber evaluated the intermediate scattering function for a translating nucleus and for a rigid rotor.

To apply the ZG formalism to thermal neutron scattering from a molecular gas, it is assumed that the molecular Hamiltonian is separable into the sum of Hamiltonians

for vibrational, rotational, and translational motion

$$H = H_{vib} + H_{rot} + H_{trans}.$$

The molecular wavefunction is then a product of wavefunctions for these motions $\psi = \psi_{vib}\ \psi_{rot}\ \psi_{trans}\ \psi_{spin}$ whence the matrix elements in II-29 separate. The vibrational and translational terms are evaluated using the ZG results. The rotational term is found using Rahman's (1961) technique, in which the rotational wavefunction is expanded in terms of symmetric top wavefunctions, the matrix elements evaluated using the properties of these wavefunctions, and the results averaged over molecular orientations. In this treatment, it is assumed that the averaging over molecular orientations may be performed separately for the rotational and vibrational terms. Griffing (1961) has derived analytic expressions for the double differential cross section of methane for the case in which correlations between nuclear spins are neglected.

Spin effects may be included in this formalism through the use of the effective (spin dependent) scattering lengths introduced in section 2 and the use of properly symmetrized wavefunctions. Zemach and Glauber showed that the effect of correlations between nuclear spins is to introduce an additional contribution to the interference term. They also showed that the effects of spin correlations in the molecule became important only at very low temperatures.

Analytic expressions for the double differential cross section of methane gas including the effects of correlations between the hydrogen spins and considering rotational

levels up to J = 4 have been obtained by Sinha and Venkataraman (1966). The expressions are formidable.

A computationally more convenient expression for the total cross section of methane has been derived by Krieger and Nelkin (1957). The expression is valid when:

(1) correlations between nuclear spins are neglected

(2) the incident neutron energy E_o is much larger than the separation between rotational energy levels

(3) the temperature T is much larger than the rotational constant.

The expression is

$$\sigma = \sigma_{free} \frac{2\omega}{E_o} \{erf(C^{\frac{1}{2}}) - (1 - p)^{\frac{1}{2}} \exp(-Cp)\ erf[C^{\frac{1}{2}}(1-p)^{\frac{1}{2}}]\} \qquad \text{II-31}$$

where

σ_{free} is the free-proton cross section (20.38 barns)

ω is the energy of the lowest normal mode vibration (0.1656 ev)

T is the temperature in ev

erf(Z) is the error function, $erf(Z) = \frac{2}{\sqrt{\pi}} \int_o^Z \exp(-x^2)\,dx$

$C = \frac{E_o \bar{m}}{T}$

$p = (1 + \alpha^2/\beta)^{-1}$

$\alpha = (1 + \bar{m})/T$

$\beta = \bar{m}/(2\omega T)$

and $\bar{m}$ is the ratio of the neutron mass to an effective mass which describes the effects of chemical binding (Sachs and Teller 1941; Messiah 1951). $\bar{m} \simeq 0.2944$.

Since the rotational constant of methane is 5.225 $cm.^{-1}$ (Herzberg 1945), the KN approximation is valid for temperatures $T>>7.51^{o}K$. Measured total cross sections at $85^{o}K$ and $20.4^{o}K$ are in reasonable agreement with the results of KN calculations (Whittemore 1964; Rogalska 1965).

The temperature dependence of the total cross sections calculated for the neutron wavelengths used in the experiment using equation II-30 is given in table II-2.

TABLE II-2

The temperature dependence of the total cross section of methane calculated using the Krieger-Nelkin expression and the neutron wavelengths used in the experiment. The cross sections are given in barns.

$T(^{o}K)$	λ = 1.06Å	λ = 1.74Å	λ = 4.70Å
10	151.4	177.3	198.2
20	151.4	177.8	204.3
30	151.4	178.2	210.4
40	151.4	178.7	216.5
50	151.4	179.1	222.5
60	151.4	179.6	228.4
70	151.4	180.0	234.2
80	151.4	180.5	239.9
90	151.4	181.0	245.5
100	151.4	181.4	251.0

The preceding calculations for the dependence of the total scattering cross section of methane upon the average spin quantum number I is strictly valid only at very long wavelengths, while the experiments reported here were done at wavelengths from 1.06 to 4.70Å. One therefore has doubts as to whether the effect of spin species conversion on the total cross section will be as large as theory predicts, or in fact, whether the effect will be observable at all.

We are guided by the case of ortho-para conversion in hydrogen, where the total cross section of both the ortho- and para- species have been measured as a function of neutron wavelength at 20.4°K (Whittemore 1964). At 4.70Å, the total cross sections of the two spin species differ by more than a factor of ten, and at 1.74Å they differ by more than a factor of two. At 1.06Å, the difference is rather small (~1-2 barns). One would expect the case of methane to be qualitatively similar, with the magnitude of the change scaled down somewhat because of the larger dimensions of the methane molecule. Even after allowing for only partial conversion, we expect that the changes in the cross sections measured at the above wavelengths should be easily observable.

CHAPTER III

APPARATUS AND MEASUREMENTS

1. Introduction

In the preceding chapter it was shown that changes in the relative populations of nuclear spin symmetry species in methane would manifest themselves as time-dependent changes in the total elastic scattering cross section for slow neutrons. In this chapter we describe experiments to observe and to study the conversion between spin symmetry species in solid methane through measurements of the total scattering cross section.

The total cross sections were determined from measurements of the transmission of a beam of thermal neutrons through a planar slab of solid methane of known thickness. This is the simplest possible geometry for total cross section measurements; the number of neutrons transmitted through the specimen is given by the expression

$$n = n_o \exp(-N\sigma t) \qquad \text{III-1}$$

where n is the number of neutrons transmitted through the sample

n_o is the number of neutrons incident on the sample

N is the number of molecules per unit volume

σ is the total cross section per molecule

and t is the thickness of the sample.

The total cross section was measured at incident neutron wavelengths of 1.06, 1.74 and 4.70Å as a function of temperature from 4.2 to 100°K and as a function of time upon rapid cooling to 4.2°K.

In this chapter we shall briefly describe the apparatus used to make these measurements, paying particular attention to the specimen chamber, and then describe the measurements themselves.

2. Apparatus

The physical properties of methane, the use of a transmission geometry with a plane slab sample, and the necessity of working at very low temperatures to induce nuclear spin conversion placed severe constraints on the design of the experiment. These constraints were most evident in the design of the sample chamber and included:

(1) in order to measure the cross section accurately, rather thick samples had to be used (a sample thickness of 0.31 cm.was required to reduce the beam intensity by a factor of (3/2)e)

(2) the sample chamber must be vacuum tight at liquid helium temperatures

(3) the material of which the sample chamber was constructed must be machinable to very fine tolerances and must be capable of maintaining these tolerances without warping or deforming upon repeated cycling from room temperature to liquid helium temperature under conditions of high vacuum.

(4) the empty chamber must transmit at least 80% of the incident neutrons

(5) the sample chamber should use the maximum amount of the incident neutron beam area, subject to the size restrictions imposed by the dimensions of the cold chamber of the cryostat.

(6) a small low temperature thermal expansion coefficient for the chamber material was desirable.

(7) the material should have good thermal conductivity

(8) provision must be made for safely introducing and removing the methane sample.

Number 304 stainless steel was used as the construction material for the sample chamber, primarily because it could be machined thin enough to satisfy constraint #4 while still satisfying #3, and, to a lesser extent, #6 and #7.

The sample chamber is sketched in figure III-1. The requirements that the vertical surfaces be exactly parallel and that the sample thickness be known to less than 0.001 inch, together with the two inch depth of the chamber, meant that the sample chamber had to be constructed in two pieces which were then joined together using stainless steel screws with an indium vacuum seal in the joint. The outer dimensions of the assembled chamber were measured with a micrometer before and after the insertion of the indium seal so that the specimen thickness was precisely known. Another indium seal was required where the brass inlet/outlet tube joined the sample chamber. To avoid subjecting the thin-walled sample chamber to high

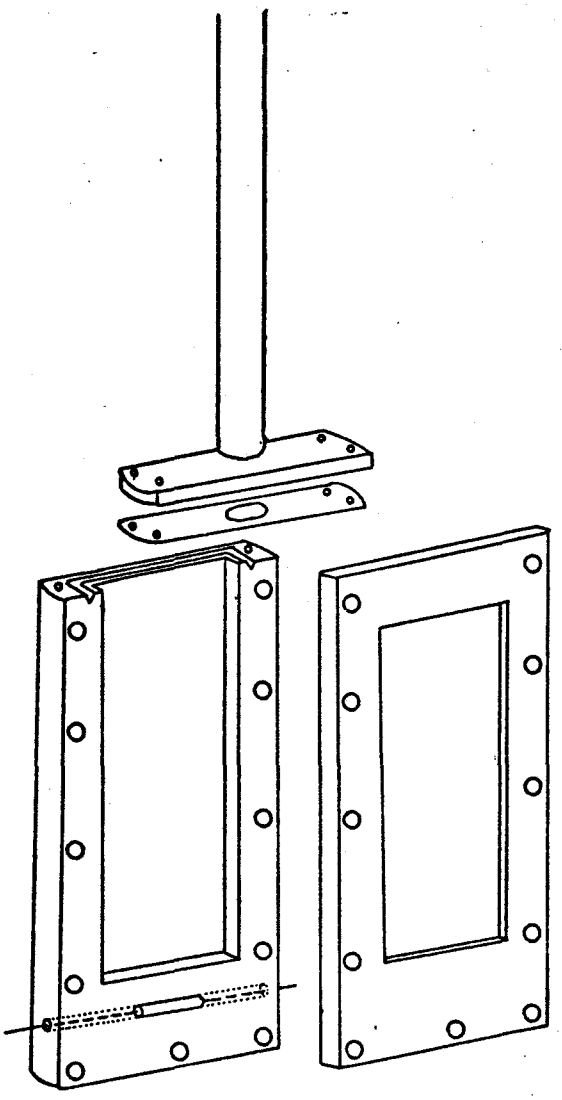

Figure III-1 An exploded view of the sample chamber. The chamber was constructed of stainless steel with thin (0.040 inch) windows for the neutron beam. The carbon resistance thermometer was mounted in the base. Indium vacuum seals were used in all joints. The drawing is actual size.

pressure as the methane vaporized at the end of the experiment, the inlet tube was provided with a heating coil that ensured that the sample always thawed first at the inlet/outlet hole and that the inlet tube did not become blocked with solid methane. Thermal insulation between the tube and the rest of the scattering chamber was provided by a sheet of 0.005 inch thick stainless steel. This necessitated another indium seal. Two sample chambers were used in the experiments, both with transmissions of about 0.40 when filled with solid methane. The assembled chambers were vacuum tested on a helium leak detector and were found to be vacuum tight at 77°K. The large surface area of the sample chamber in contact with the cold helium exchange gas allowed rapid cooling of the methane sample.

The heating coil mentioned above consisted of sixteen feet of #32 gauge constantan wire wound non-inductively about the brass tube. The resistance of the coil was about 45 ohms. Thermal contact between the coil and the tube was provided by General Electric G1202 glyptol varnish. A 500 ohm ½ watt current-limiting resistor was placed in series with the coil. Power was provided by a variac.

The most important use of the heating coil proved not to be the function described above, but rather in getting the methane into the sample chamber. The sample chamber was to be filled by admitting methane gas to the cold, evacuated system and allowing the gas to condense and run down into the chamber. However, methane is a liquid only in the narrow range from 91 - 111°K. It was found that with only the liquid

nitrogen tanks of the cryostat filled, the lowest temperature reached at the sample chamber was about 120°K, while with liquid helium in the cryostat, the methane solidified along the inlet tube. The heating coil was useful in keeping the methane liquid along the inlet tube. To monitor the temperature along the inlet tube, a copper-constantan thermocouple was placed in contact with the tube one-half way along its length.

The cryostat used in these experiments was constructed by Sulfrian Cryogenics, Inc. The tail assembly was constructed of aluminum and had thin-walled "windows" (0.015 inch thick) through which the neutron beam passed.

Another major piece of equipment was the vacuum/methane delivery system, indicated schematically in figure III-2. In actuality these were two separate systems which were coupled only during the experiment; the requirement of portability dictated this arrangement. The best vacuum measured with the Pirani gauge P2 under experimental conditions was about 1×10^{-3} torr.

Initially valves V1, V2, V3 and V4 would be open and the sample chamber evacuated until the desired pressure, measured at P2, was obtained. Then the methane transfer system would be isolated by closing valves V2 and V3. The regulator R and the valve V1 were used to control the flow of methane from the gas cylinder M to the glass storage vessel C. The latter was designed so that the volume of methane gas that it held at STP would completely fill the sample chamber at 20°K.

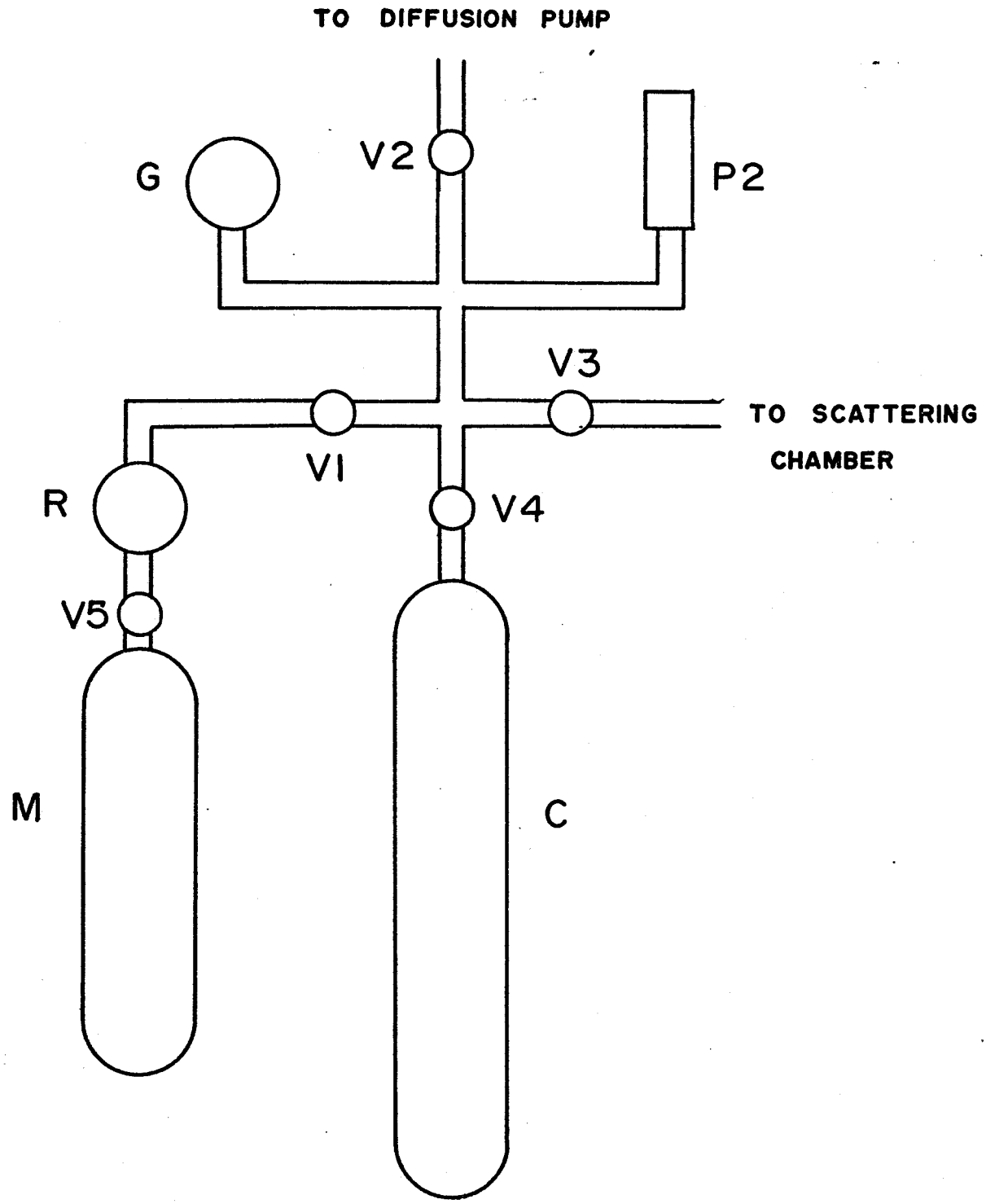

Figure III-2 A schematic diagram of the vacuum/methane transfer system. The symbols are explained in the text.

When atmospheric pressure was read on the gauge G, the flow of gas was stopped and the valve V3 opened, admitting the methane gas to the sample chamber.

The specimens used in these experiments were condensed from research grade methane gas (Matheson of Canada, Whitby, Ontario) of 99.98 molar per cent nominal purity. No attempt was made to purify the gas further. The probable impurities were ethane, carbon dioxide, and air. Evacuating the system to a pressure of less than 1×10^{-2} torr before transferring the methane gas limited additional impurities to less than 160 ppm of air. The total oxygen impurity was probably less than 60 ppm.

A 56 ohm, one-eighth watt "Ohmite" carbon composition resistor was used as a resistance thermometer to determine the sample temperature. The thermometer was mounted in the base of the sample chamber about one-quarter of an inch from the methane. Thermal contact between the chamber and the thermometer was provided by Apiezon vacuum grease. A four terminal arrangement was used to measure the resistance, with the voltage across the resistor being measured on a Keithley model 160 multimeter. The current through the resistor was determined by measuring (on a Hewlett-Packard model 3420A differential voltmeter) the voltage across a General Radio 1×10^{6} ohm resistance standard in series with the resistor. The voltage source was a pair of Eppley student standard cells connected in series. Measurements were taken in both current directions to eliminate thermal emfs.

The temperature dependence of resistors of this type may be fitted to a three parameter equation of the form

Figure III-3

A general view of the experiment. The methane transfer system is at the left and the cryostat at the centre. A part of the detector appears at the lower right. The large frame was used to lift the cryostat out of the neutron beam during the experiment. The neutron beam tube and the incident beam collimator are visible immediately behind the tail of the cryostat.

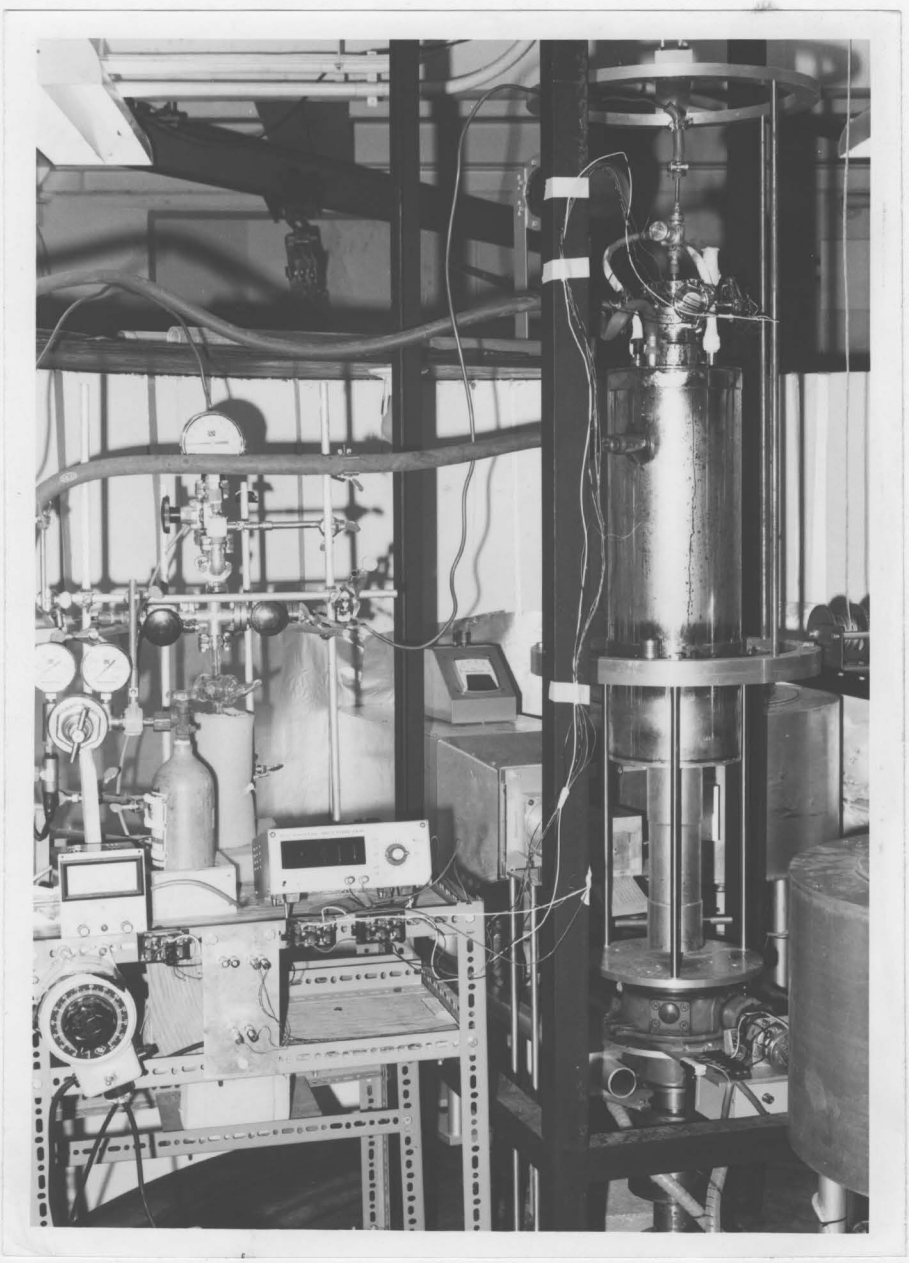

(Clements and Quinnell 1952)

$$\log_{10}R + \frac{C}{\log_{10}R} = A + \frac{B}{T} \qquad \text{III-2}$$

where R is the thermometer resistance and T is the temperature in ^{o}K. The thermometer was calibrated by measuring the resistance at 4.2, 77 and 194.7^{o}K and solving for the parameters A, B and C. The accuracy of the calibration was estimated to be about $\pm 0.2^{o}K$ in the immediate vicinity of $4.2^{o}K$ and $\pm 1.0^{o}K$ elsewhere.

In order to make measurements with the sample successively in and out of the neutron beam, a frame to which a small winch was attached was constructed to permit the cryostat to be raised out of the beam. Since the cryostat support had several three-quarter inch projections on its lower surface which fit into cuts on the specimen table of the spectrometer, the orientation of the sample with respect to the neutron beam was not changed by raising and lowering the cryostat.

The apparatus is illustrated in figure III-3.

3. Measurements

All the measurements reported in this work were made on the triple-axis spectrometer (Brockhouse et al. 1968) at the McMaster University nuclear reactor. The spectrometer is illustrated in figure III-4.

Measurements were made at incident neutron wavelengths of 1.06, 1.74 and 4.70Å. The shorter wavelength incident

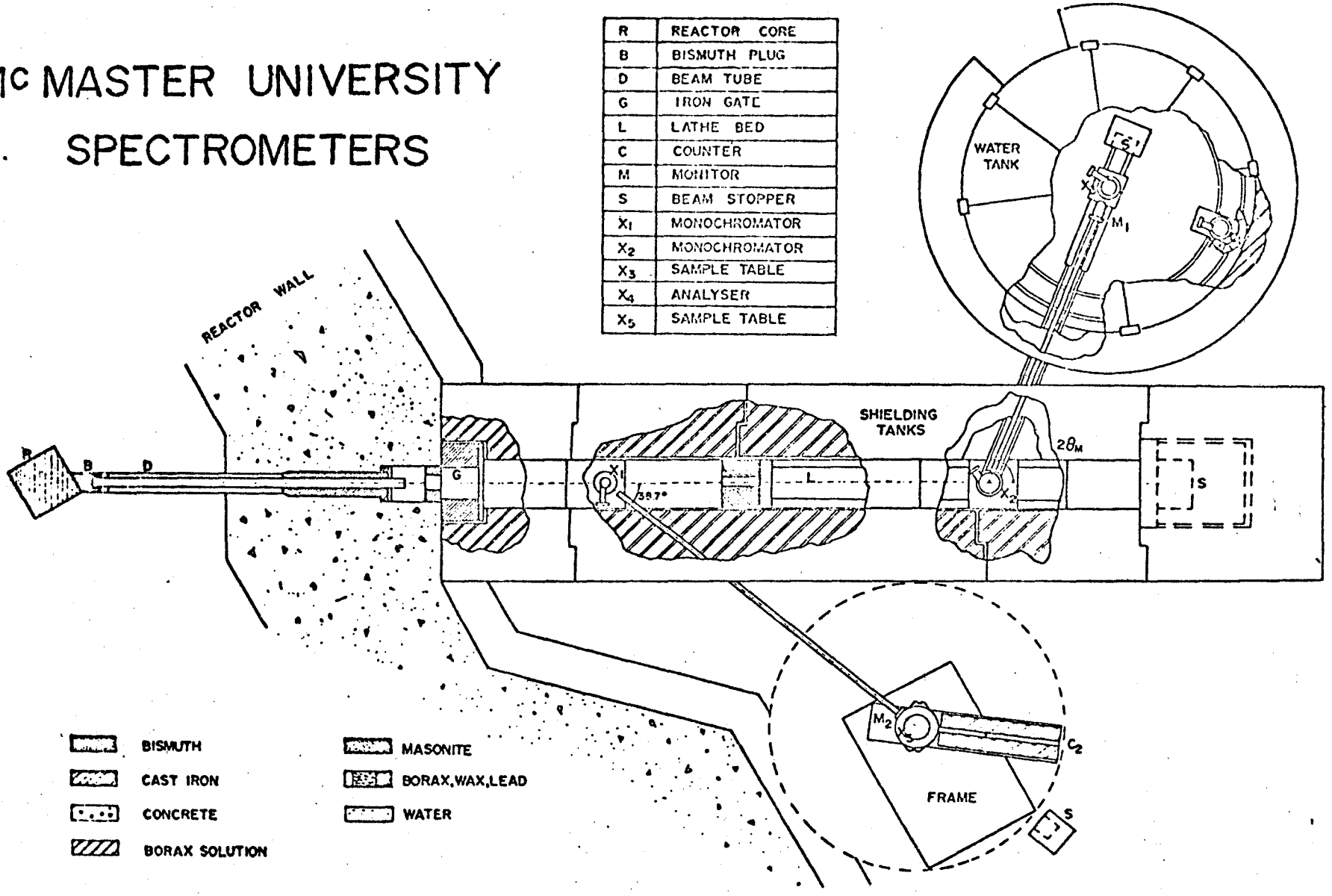

Figure III-4 The triple-axis spectrometer at the McMaster University nuclear reactor. (from Brockhouse et al. 1968)

beams were obtained from the "white" neutron beam from the reactor by Bragg reflection off the (200) and (111) planes of a large copper single crystal. The longest wavelength was obtained by Bragg reflection off the (002) planes of a pyrolitic graphite block; the beam was then passed through a four inch long beryllium filter to remove higher order contaminants.

Measurements commenced with the determination of the optimum bias voltages of the helium proportional counters used. Discrimination curves were taken for various amplifier gains and were optimized for both the monitor counter and the transmitted beam counter. The straight through position of the detector was found by rocking the transmitted beam counter about the calculated zero angle. The incident beam collimator was aligned so that its centre lay precisely along the line of join, passing over the centre of the specimen table, between the centre of the detector and the centre of the beam tube. Horizontal and vertical Soller slits with angular divergences of 22 minutes of arc were used to collimate the transmitted beam. The position of the monitor counter and the size of the collimated incident neutron beam were adjusted so that monitor and detector count rates were about 1000 counts per second. The fast neutron component of the beam was measured by placing several thicknesses of 0.020 inch cadmium sheet before the Soller slits. The location of the edges of the scattering chamber were determined at liquid nitrogen temperatures and the incident beam collimator adjusted such that the beam passed through the sample area. The transmission of the evacuated sample chamber was measured at liquid nitrogen temperatures and the required amount of methane was

subsequently condensed into the scattering chamber.

The monitor scaler was preset to 4×10^4 counts (4×10^3 counts for the 4.70Å beam) and a gate pulse from it was used to stop the detector scaler. Counts were taken while the liquid helium was being transferred but during this time the sample could not be lifted up out of the beam. Temperature and time measurements were made near the end of each counting period.

The sample slowly cooled to a temperature of about $20^\circ K$ and then rapidly cooled to $4.2^\circ K$. Once the transfer of helium was completed, the sample could be removed from the beam and subsequent measurements were made for the most part with the sample alternately in and out of the beam. Transmission measurements were made for periods of several hours after rapid cooling of the sample to $4.2^\circ K$ in order to observe the effects of spin conversion.

In some experiments, after the sample had been held at a temperature of $4.2^\circ K$ for several hours, it was allowed to warm to about $20^\circ K$ and then rapidly cooled once more.

CHAPTER IV

ANALYSIS AND RESULTS

1. Calculation of the Total Scattering Cross Sections

Because of the large amounts of data to be handled in the form of the various sets of count, time and voltage measurements, the calculation of the temperatures and cross sections from the raw data was done on a CDC 6400 computer. The computer program subtracted the fast neutron background, calculated the temperature from the various sets of voltages, distinguished between "sample in" and "sample out" counts, made corrections in the thickness of the sample and in the number of molecules per unit volume using the thermal expansion data of Manzhelii et al.(1969) and Heberlein and Adams (1970), calculated the transmission of the scattering chamber from the experimental data and removed it from the methane transmission, calculated the total cross section using equation III-1, and subtracted the absorption cross section. The cross section was calculated using the average of the "sample out" counts immediately preceding and following the given "sample in" count; if one of these was missing, then the mean of all the "sample out" counts was used in its place. No corrections were made for multiple scattering since the

detector was tightly collimated and was located several feet from the sample.

The error in the total scattering cross section was estimated using the expression

$$\left|\frac{\Delta\sigma}{\sigma}\right| = \left(\left| \frac{\Delta n}{n \ \ell n(n/n_o)} \right|^2 + \left| \frac{\Delta n}{n_o \ \ell n(n/n_o)} \right|^2 + \left| \frac{\Delta t}{t} \right|^2 \right)^{\frac{1}{2}} \qquad \text{IV-1}$$

where the error in the counts n and n_o was the statistical uncertainty ($\sqrt{n}$) in random counting events.

2. Temperature Dependence of the Total Scattering Cross Sections

The variation of the total scattering cross section of methane with temperature in the range from 5^o to 100^oK was examined in detail at incident neutron wavelengths of 1.06Å and 1.74Å. The experimental results are summarized in tables IV-1 and IV-2 and in figures IV-1 and IV-2.

The total scattering cross section measured at 1.74Å decreased linearly with decreasing temperature for the range from 90^oK to ~ 20^oK, but showed abrupt changes at the solid-liquid transition and at the upper (20.4^o) phase transition. The cross section decreased more or less linearly with decreasing temperature below the upper phase transition, but showed no abrupt change at the lower (8^o) phase transition. Various functions were least squares fitted to the experimental data, with the best fits in the regions above and below the upper λ-transition being given by the following straight lines:

$$\sigma(T) = 142.2 + 0.0546T \qquad (21^o<T<90^o\text{K})$$

$$\sigma(T) = 138.5 + 0.171T \qquad (6^o<T<21^o\text{K}).$$

Figure IV-1

The temperature dependence of the total scattering cross section of methane measured at an incident neutron wavelength of 1.06Å. The dashed line is the best least-squares fit of a straight line to the data. The solid circle at 4.2°K is the average of many measurements. The increase in the cross section value below ~5°K is evidence of spin species conversion.

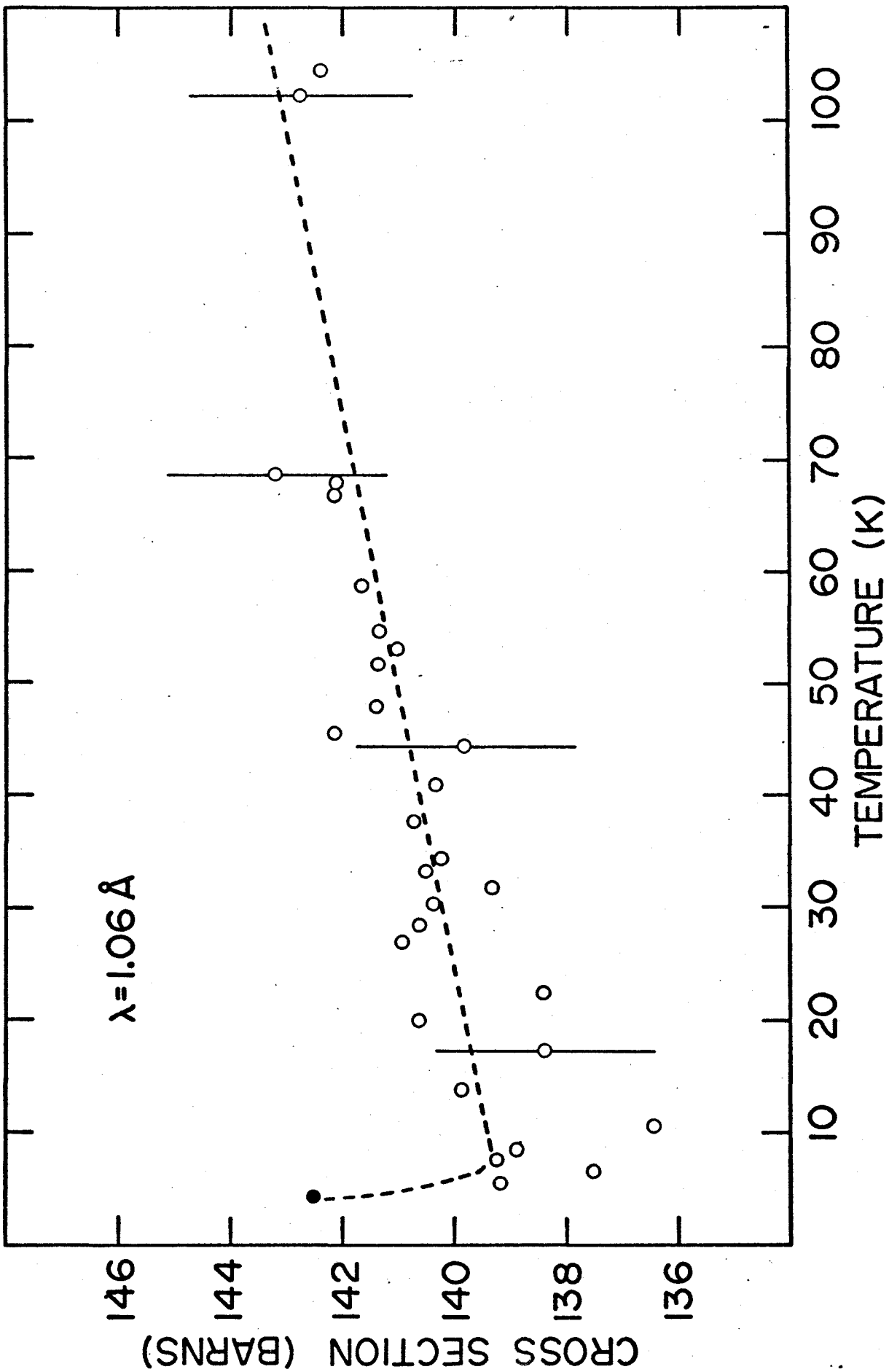
λ=1.06 Å
CROSS SECTION (BARNS)
146
144
142
140
138
136
TEMPERATURE (K)
10
20
30
40
50
60
70
80
90
100

TABLE IV-1

The measured temperature dependence of the total scattering cross section of solid methane at an incident neutron wavelength of 1.06Å

Temperature (°K)	σ (barns)
104.2 ± 1.00	142.4* ± 1.7
102.4	142.9*
68.3	143.2
67.4	142.1
66.6	143.2*
58.5	141.7
54.3	141.3
52.7	141.0
51.6	141.4
47.8	141.4
46.5	142.2
45.3	142.2
44.1	139.8*
41.0	140.4
37.7	140.8
34.4	140.3
33.3	140.5 ± 1.6
31.6	139.3
30.1	140.4
28.6	140.7
26.8	140.9
24.8	142.4
22.3	138.4
20.0	140.7
17.4	138.4
13.7	139.9
10.5	136.4
8.4	138.9
7.9	138.8
6.6	137.5*
5.7	139.3
4.2 ± 0.2	142.6*

*average of several measurements

Figure IV-2

The temperature dependence of the total scattering cross section of methane measured at an incident neutron wavelength of 1.74Å. The dashed line is merely a guide to the eye. Abrupt changes in the total cross sections are seen ~90°K and 20°K. The solid circle at 4.2°K is the average of many measurements; the increase in the cross section below ~5°K clearly shows the effect of spin conversion.

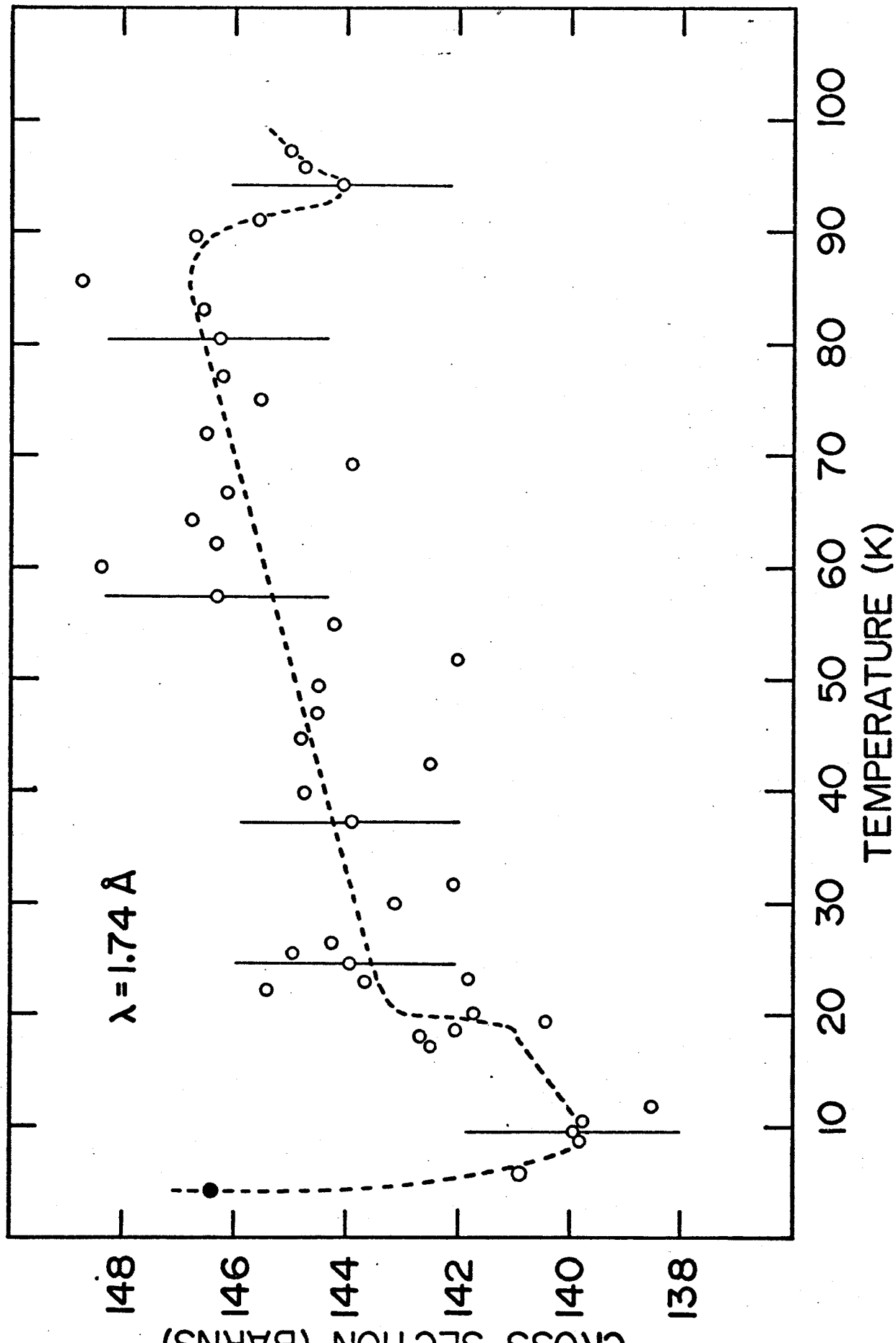
λ = 1.74 Å
CROSS SECTION (BARNS)
148
146
144
142
140
138
TEMPERATURE (K)
10
20
30
40
50
60
70
80
90
100

TABLE IV-2

The measured temperature dependence of the total scattering cross section of solid methane at an incident neutron wavelength of 1.74Å

Temperature (^{o}K)	σ (barns)
97.2 ± 1.0	145.0 ± 1.7
95.5	144.8*
94.0	144.1
90.9	145.6
89.5	146.7
86.7	140.5
85.4	148.7
82.8	146.6
80.4	146.3
77.0	146.2
74.9	145.5
71.9	146.5
69.2	143.8
66.6	146.2
64.2	146.8
62.0	146.3
59.9	148.4
57.3	146.4
54.9	144.2
51.6	142.0
49.2	144.5
46.9	144.5
44.5	144.8
42.3	142.5
39.7	144.7
37.1	143.9
34.4	146.1
31.8	141.9
29.4	143.2
27.7	139.9 ± 1.6
26.3	144.2
25.5	145.0
24.6	143.9*
24.0	143.9
23.2	141.8*
22.9	143.7*
22.1	145.4**
20.1	141.7
19.3	140.4
18.4	142.0
18.0	142.7*
17.1	142.5
11.2	138.3

Table IV-2 (continued)

10.3	139.7
9.7	139.9
8.7	139.8*
5.8	141.1*
4.2 ± 0.2	146.4*

* average of several measurements

The abrupt increase in the scattering cross section seen as the temperature decreased through the solid-liquid transition is accounted for by the increased elastic scattering (nuclear Bragg scattering) and phonon-scattering associated with the formation of a regular crystal lattice in the solid phase. A similar change in the total scattering cross section of methane at the solid-liquid transition has been observed at 6.52Å (Van Dingenen and Nève de Mevergnies 1964). The smooth decrease in the total cross section from 90°K to ~21°K probably results from decreased inelastic scattering as various vibrational and rotational modes are thermally depopulated.

The abrupt decrease in the cross section as the temperature decreased through the upper λ-transition is consistent with a change in the rotational freedom of the methane molecule to a more hindered rotational state. A change from a disordered to an ordered structure, unaccompanied by a change in the energies of the rotational modes, could not account for the observed change since one would expect

such a change to have little effect on the total cross section or to increase the total cross section because of increased elastic scattering (superlattice lines). The more or less linear decrease of the total cross section below $20^{o}K$ is probably the result of the freezing out of vibrational and rotational modes.

A comparison of the slopes of the straight line fits to the data in the regions above and below the upper phase transition is consistent with the molecular rotation being more strongly hindered below the transition. The higher slope value below the transition suggests that the excitations are of higher energy in that region (i.e. - the free rotation of the molecule is more strongly hindered). This would be consistent with the shift in the 12 mev band in the frequency spectrum of methane towards higher energies at lower temperatures observed by Dorner and Stiller (1964); they identified this peak with rotational modes.

The values of the total cross sections measured in this work are somewhat smaller (~10%) than those predicted by the free rotation Krieger-Nelkin approximation. The KN expression was least-squares-fitted to the experimental data in the region from $21^{o}K$ to $90^{o}K$ where it is most likely to be valid, treating the effective mass ratio $\bar{m}$ (which describes the effects of chemical binding on the scattering) as a free parameter. The best fit was obtained with a value of $\bar{m} = 0.454 \pm 0.018$, or $m_{eff} = 2.2 \pm 0.1$ neutron masses. This agrees well with the value of $m_{eff} = 2.1$ neutron masses obtained by Janik

(1965) in fitting to the energy dependence of the differential cross section at ~85°K.

The total cross section measured at 1.06Å decreased linearly with decreasing temperature and showed no change within error at the upper λ-transition. The best fit to the data was the following straight line:

$$\sigma(T) = 139.1 \pm 0.0399T \qquad (6^{\circ} < T < 100^{\circ}K).$$

The cross sections measured at 1.06Å are in somewhat closer agreement with the results of a KN calculation. The best fit of the KN formula to the data yielded a value of $\bar{m} = 0.360 \pm 0.020$ ($m_{eff} = 3.0 \pm 0.1$ neutron masses). The better agreement with the KN approximation and the smaller σ/T slope value of the 1.06Å data may be explained by considering the energy of the neutrons. The energy of the 1.06Å neutrons is large compared to both that of the 1.74Å neutrons (72.8 mev as opposed to 27.0 mev) and to the rotational level separations. Because of its high energy, a 1.06Å neutron is able to excite rotational and vibrational modes whose populations have been thermally depleted. Because much of the inelastic scattering is from neutron energy loss processes, thermal depopulation of energy levels and increases in mode energies through increased rotational hindering have less effect on the inelastic scattering, with the result that changes in the total scattering cross section with temperature are less pronounced.

3. Spin Conversion

The total scattering cross section measured at 1.74Å and 4.70Å showed anomalous changes upon rapid cooling

Figure IV-3

The total scattering cross section of methane measured at an incident neutron wavelength of 1.74Å upon rapid cooling to 4.2°K. The solid circles at times from 0 to ~18 minutes are measurements taken as the sample cooled from ~20°K to ~6°K; the empty circles are measurements taken at 4.2°K at times after 18 minutes. The increase in the cross section resulting from spin species conversion is clearly evident.

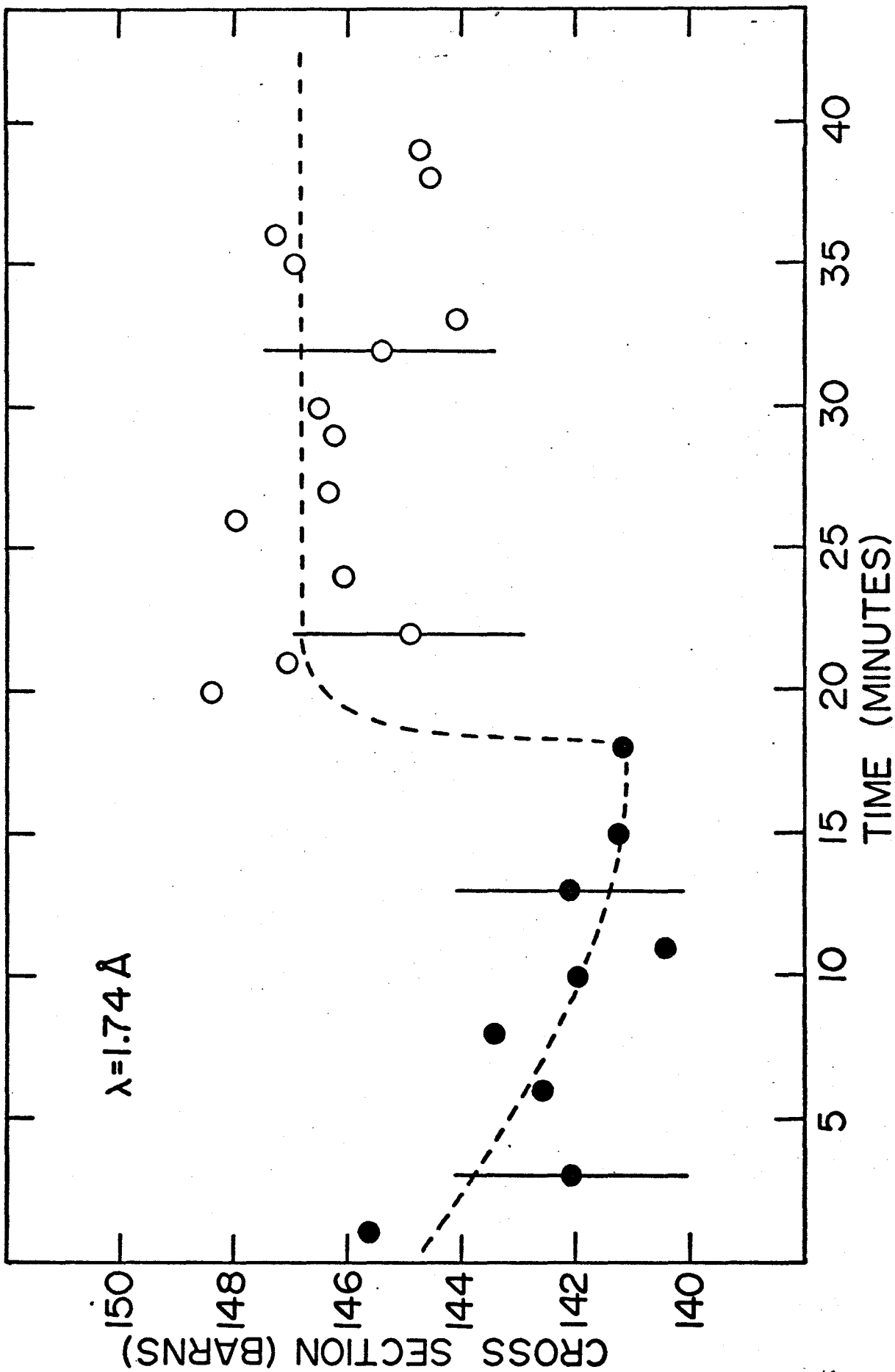
λ=1.74 Å
CROSS SECTION (BARNS)
150
148
146
144
142
140
TIME (MINUTES)
5
10
15
20
25
30
35
40

($\lesssim 2^{o}K$/minute) to $4.2^{o}K$. The data are given in figures IV-3 and IV-4. Initially the cross section continued to decrease as the sample cooled from $\sim 20^{o}K$. By the time the sample temperature reached $4.2^{o}K$ (or had been at $4.2^{o}K$ for a few minutes) the cross section increased to approximately its $90^{o}K$ value. At both wavelengths the change in the cross section was of the order of 8 barns. The time constant for the conversion process was too short to be measured reliably; it was certainly less than 20 minutes. The short time constant suggests that the sample may have contained more than the estimated 60 ppm of oxygen. The curves of figures IV-3 and IV-4 resemble those obtained by van Hecke et al.(1972) in NMR studies on methane containing ~1 molar % of oxygen impurity.

If we assume that the total inelastic scattering cross section measured at $4.2^{o}K$ is not significantly changed by conversion between spin species, then the change in the $\langle I(I+1)\rangle$ value can be calculated from equation II-22. The resulting expression, valid at constant temperature, is

$$\Delta[\langle I(I+1)\rangle] = \frac{\Delta\sigma}{\pi(b_{(+)} - b_{(-)})^2} \qquad \text{IV-2}$$

To compute numerical values of $\langle I(I+1)\rangle$ from the experimental data, we need the value of the unconverted cross section at $4.2^{o}K$. In the case of the data obtained at 1.74Å, this value was obtained by extrapolating the straight line fit to the cross section versus temperature curve measured below $20^{o}K$ to

Figure IV-4

The total scattering cross section of methane measured at an incident neutron wavelength of 4.70Å upon rapid cooling to 4.2°K. The solid circles at times from 0 to ~17 minutes are measurements taken as the sample cooled from ~20°K to ~6°K; the empty circles are measurements taken at 4.2°K at times after 17 minutes. The increase in the cross section resulting from spin species conversion is clearly evident.

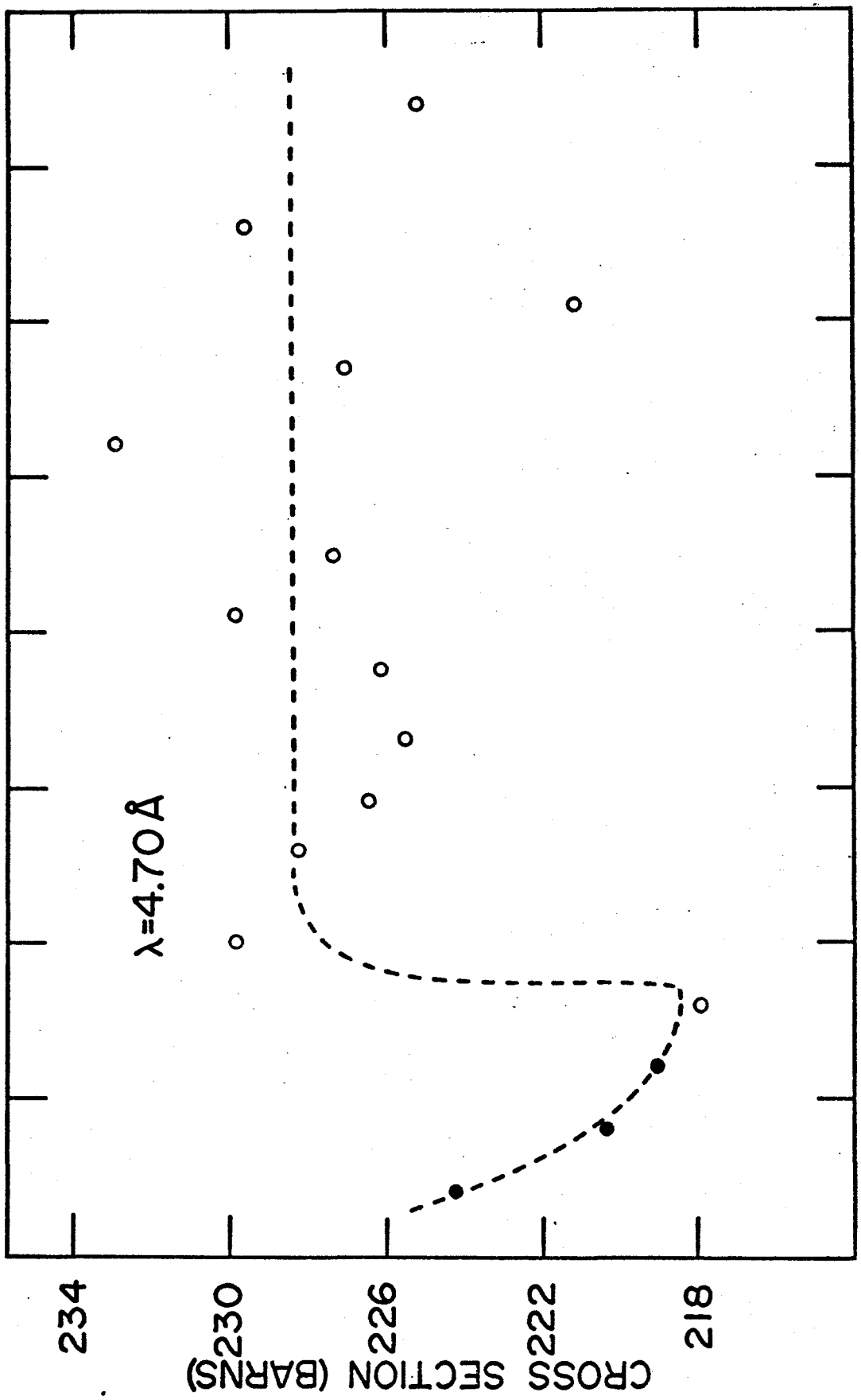
λ=4.70 Å
CROSS SECTION (BARNS)
234
230
226
222
218
10
20
30
40
50
60
70
TIME (MINUTES)

4.2°K. The extrapolated value is identical within the experimental error to the cross section values measured near 11°K; the error introduced by using the extrapolated value is probably less than the error in the individual absolute cross section measurements. For the data obtained at 4.70Å, the value of the cross section measured at 4.2°K before the abrupt increase was used as the unconverted value. It should be noted that although the error in the absolute cross sections measured at 4.70Å was rather large (±6.4 barns) the error in the relative cross sections was much smaller (± 3.2 barns). Thus the error in the calculated value of $\langle I(I+1)\rangle$ was reasonably small.

The average values of the change $\Delta[\langle I(I+1)\rangle]$ obtained at 1.74Å and at 4.70Å were 0.068 ± 0.018 and 0.097 ± 0.038 respectively. Both these values represent averages of more than 50 measurements. Using the constant value of $\langle I(I+1)\rangle = 3.25$ measured in the region from 40°K to 20°K (Bloom and Morrison 1972) as our initial value, we find that at 4.2°K, the equilibrium value of $\langle I(I+1)\rangle$ is 3.33 ± 0.020. This value is considerably less than the value of ~3.70 ± 0.18 obtained by Wong et al. (1969), Piott (1971), and van Hecke et al. (1972) in nuclear magnetic susceptibility measurements.

The reason for this discrepancy is unclear. Conceivably, conversion from the I = 1 state to the I = 2 state could produce a large decrease in the inelastic scattering cross section as the J = 1 rotational state is depopulated. Such a change in the inelastic cross section would obscure the increase in the elastic cross section and would lessen the

calculated $\langle I(I+1)\rangle$ value. A decrease in the inelastic cross section because of depopulation of the J = 1 rotational level is reasonable at the 1.74Å and 4.70Å wavelengths since most of the inelastic scattering at 4.20°K would be expected to be from J = 1 → J = 0 rotational transitions in which the neutron gains energy. However it is difficult to see how the fairly small (~20%) change in the J = 1 level population indicated by the NMR results would produce a large enough decrease in the inelastic cross section to obscure the large (~15%) expected increase in the elastic cross section since one would expect $\sigma_{elastic}$ to be much larger than $\sigma_{inelastic}$ at these very low temperatures. In spite of the discrepancy in the $\langle I(I+1)\rangle$ values, the fact that the total scattering cross section showed an anomalous increase is conclusive evidence of the occurrence of nuclear spin species conversion in solid methane at very low temperatures.

4. Conclusions

The temperature dependence of the total scattering cross section of methane has been measured in the temperature range from 4.2°K to 104°K at incident neutron wavelengths of 1.06Å and 1.74Å. The total cross sections measured at both 1.06Å and 1.74Å decreased linearly with decreasing temperature over most of the range. The cross sections measured at 1.74Å showed abrupt changes at the solid-liquid transition and at the upper λ-transition. The change at the λ-transition is interpreted as a change in the rotational freedom of the molecules to a more hindered state below the transition. The relative values of the slope of the σ versus T curves above and below

the transition also support this conclusion. The best fits of the Krieger-Nelkin formula to the data were obtained with m_{eff} values of 3.0 ± 0.1 neutron masses at 1.06Å and 2.2 ± 0.1 neutron masses at 1.74Å. The latter value is in good agreement with that obtained by Janik (1965) at long wavelengths.

The total scattering cross sections measured at 1.74Å and 4.70Å showed anomalous changes upon rapid cooling to 4.2°K, the cross section increasing to approximately its 85° - 90°K value. The time constant for the change was very short (certainly < 20 minutes). The increase in the cross section is evidence of conversion between nuclear spin species in methane. The mean change in $\langle I(I+1)\rangle$ was calculated to be 0.083 ± 0.020. Thus, the equilibrium value of $\langle I(I+1)\rangle = 3.33$ at 4.2°K. This value is considerably smaller than those (~3.70) obtained in NMR experiments. The discrepancy in the values obtained by the two techniques may be the result of changes in the inelastic neutron scattering cross section which were assumed to be small in the calculation of $\langle I(I+1)\rangle$. Our measurements provide an independent confirmation of the existence of nuclear spin species conversion in CH_4 at very low temperatures.

BIBLIOGRAPHY

S. Alexander and M. Lerner-Noar, Can. J. Phys. 50 (1972)1568

G. E. Bacon, Neutron Diffraction (Oxford University Press, Oxford 1962)

A. Bajorek, I. Natkaniec, K. Parlinski, M. Sudnik-Hrynkiewicz, J. A. Janik, J. M. Janik, K. Otnes and E. Tunkels, Molecular Dynamics in Gaseous and Solid Methane (Institute of Nuclear Physics Report 608/PS, Cracow, 1968)

E. A. Ballik, D. J. Gannon and J. A. Morrison, J. Chem. Phys. 57 (1972) 1793

M. Bloom and E. P. Jones, Phys. Rev. Letters 8 (1962)170

M. Bloom, Proceedings of the IVth International Magnetic Resonance Conference (1971) to be published.

M. Bloom and J. A. Morrison, Specialist Periodical Reports, Vol. II (The Chemical Society, London, 1972) to be published

L. B. Borst, S. L. Borst, L. Koysooko, H. Patel and E. Stusnick, Phys. Rev. Letters 7 (1961)343

L. B. Borst, Fundamental Liquids (Twin Bridge Press, Williamsville, New York, 1971).

B. N. Brockhouse, S. Hautecler, and H. Stiller in The Interaction of Radiation with Solids, ed. by R. Strumane, J. Nihoul, R. Gevers and S. Amelinckx (North Holland Publishing Co., Amsterdam, 1964)580

B. N. Brockhouse, G. A. deWit, E. D. Hallman, and J. M. Rowe, in Neutron Inelastic Scattering, Vol. II, (International Atomic Energy Agency, 1968) 259

J. R. Clements and E. H. Quinnell, Rev. Sci. Inst. 23, (1952)213

J. H. Colwell, E. K. Gill and J. A. Morrison, J. Chem. Phys. 36, (1962)2223

J. H. Colwell, E. K. Gill and J. A. Morrison, J. Chem. Phys. 39, (1963)635

M. F. Crawford, H. L. Welsh, and J. H. Harrold, Can. J. Phys. 30 (1952)81

G. A. deWit and M. Bloom, Can. J. Phys. 47, (1969)1195

B. Dorner and H. Stiller, Phys. Stat. Sol. 5, (1964)511

B. Dorner and H. Stiller, in Inelastic Scattering of Neutrons in Solids and Liquids, Vol. II (International Atomic Energy Agency, Vienna, 1965)291

F. H. Frayer and G. E. Ewing, J. Chem. Phys. 48, (1968)781

S. C. Greer and L. Meyer, Z. Angew. Phys. 27,(1969)198

G. W. Griffing, in Inelastic Scattering of Neutrons in Solids and Liquids, Vol. I,(International Atomic Energy Agency, Vienna, 1963)435

I. I. Gurevich and L. V. Tarasov, Low-Energy Neutron Physics, American Elsevier Publishing Co., New York, 1968).

Y. D. Harker and R. M. Brugger, J. Chem. Phys. 46 (1967)2201

S. Hautecler and H. Stiller, in Inelastic Scattering of Neutrons in Solids and Liquids,Vol. II, (International Atomic Energy Agency, Vienna, 1963)281

D. C. Heberlein and E. D. Adams, J. Low Temp. Phys. 3,(1970)115

J. Herczeg and R. E. Stoner, J. Chem. Phys. 54 (1971)2284

S. B. Herdade in Neutron Inelastic Scattering, Vol. II, (International Atomic Energy Agency, Vienna 1968)197

G. Herzberg, Infrared and Raman Spectra of Polyatomic Molecules (D. Van Nostrand Company, New York, 1945)455

H. P. Hopkins, P. L. Donoho and K. S. Pitzer, J. Chem. Phys. 47 (1967)864

D. J. Hughes and R. B. Schwartz, Neutron Cross Sections (Brookhaven National Laboratory Report BNL-325, 2nd ed., 1958)

J. Janik, Acta Phys. Polonica 27 (1965)491

J. A. Janik, in Inelastic Scattering of Neutrons, Vol. II (International Atomic Energy Agency, Vienna 1965)243

J. A. Janik, in Theory of Condensed Matter (International Atomic Energy Agency, Vienna, 1968)577

J. A. Janik, K. Otnes, G. Solt, and G. Kosaly, Discussions Faraday Soc. 48, (1969)87

Y. Kataoka and T. Yamamoto, Prog. Theor. Phys. supplement extra number (1968)436

G. Kosaly and G. Solt, Physica 32 (1966)1571

T. J. Krieger and M. S. Nelkin, Phys. Rev. 106 (1957)290

V. G. Manzhelii, A. M. Tolkachev and V. G. Gavrilko, J. Chem. Phys. Solids 30 (1969)2759

W. Marshall and S. W. Lovesey, Theory of Thermal Neutron Scattering, (Oxford University Press, Oxford, 1971)

A. M. L. Messiah, Phys. Rev. 84 (1951)204

A. M. L. Messiah, Quantum Mechanics, Vol. II, (John Wiley and Sons Inc., New York 1966)545

D. E. Parks, M. S. Nelkin, J. R. Beyster and N. F. Wikner, Slow Neutron Scattering and Thermalization (W. A. Benjamin Inc., New York, 1970)

L. Pauling, Phys. Rev. 36 (1930)430

J. E. Piott, Ph.D. Thesis, University of Washington (1971)

W. Press, J. Chem. Phys. 56 (1972)2597

M. A. Preston, Physics of the Nucleus (Addison-Wesley Publishing Co., Reading Massachusetts, 1962)26

A. Rahman, J. Nucl. Energy A13 (1961)128

Z. Rogalska, Acta Phys. Polonica 27 (1965)581

O. Runolfson, S. Mango and M. Borghini, Physica 44 (1969)494

J. J. Rush, T. I. Taylor and W. W. Havens Jr., Phys. Rev. Letters 5, (1960)507

J. J. Rush, T. I. Taylor and W. W. Havens Jr., J. Chem. Phys. 35 (1961)2265

J. J. Rush, T. I. Taylor and W. W. Havens Jr., J. Chem. Phys. 37 (1962)234

J. J. Rush, G. J. Safford, T. I. Taylor and W. W. Havens Jr., Nucl. Sci. Eng. 14 (1962)339

J. J. Rush and T. I. Taylor, J. Physical Chem. 68 (1964)2534

J. J. Rush, P. S. Leung and T. I. Taylor, J. Chem. Phys. 45 (1966)1312

R. G. Sachs and E. Teller, Phys. Rev. 60 (1941)18

G. B. Savitsky and D. F. Hornig, J. Chem. Phys. 36 (1962)2634

A. Schallamach, Proc. Roy. Soc. (London) A171 (1939)569

S. K. Sinha and G. Venkataraman, Phys. Rev. 149 (1966)1

K. Sköld, J. Chem. Phys. 49 (1968)2443

H. Stiller and S. Hautecler, in Inelastic Scattering of Neutrons in Solids and Liquids, Vol. I (International Atomic Energy Agency, Vienna, 1963)405

A. M. Tolkachev and V. G. Manzhelii, Soviet Physics- Solid State 7 (1966)1711

W. Van Dingenen and M. Neve de Mevergnies, Physica 30 (1964)237

P. van Hecke, P. Grobet and L. van Gerven, J. Mag. Resonance 7 (1972)117

R. P. Wolf and W. M. Whitney, in Proceedings of the IXth International Conference on Low Temperature Physics ed. by J. G. Daunt, D. O. Edwards, F. J. Milford and M. Yagut (Plenum Press, New York, 1965)1118

K. P. Wong, J. D. Noble, M. Bloom and S. Alexander, J. Mag. Resonance 1 (1969)55

A. C. Zemach and R. J. Glauber, Phys. Rev. 101 (1956)118,129